2010

Cathepsin B-mediated autolysosome efflux and cell death

Boram Ham

Cathepsin B-mediated autolysosome efflux and cell death

(Thesis Format: Monograph)

By

Boram Ham

Graduate Program
In
Microbiology and Immnology

Thesis submitted in partial fulfillment
Of the requirements for the degree of
Master of Science

School of Graduate and Postdoctoral Studies
The University of Western Ontario
London, Ontario

THE UNIVERSITY OF WESTERN ONTARIO
SCHOOL OF GRADUATE AND POSTDOCTORAL STUDIES

CERTIFICATE OF EXAMINATION

Supervisor	Examiners
Dr. Sung Kim	Dr. Rodney Dekoter
Supervisory Committee	Dr. Mansour Haeryfar
Dr. Joe Mymryk	Dr. Robert Cumming
Dr. Stephen Barr	

The thesis by

Boram Ham

entitled:

Cathepsin B-mediated autolysosome efflux and cell death

is accepted in partial fulfillment of the
requirements for the degree of
Master of Science

Date_____ _____
Chair of the Thesis Examination Board

ABSTRACT

Autophagy is a vesicular system which is a lysosomal degradation pathway found in organisms ranging from yeast to mammals. To date, extensive studies have unraveled the mechanism of autophagy biogenesis and more than thirty autophagy related (ATG) genes have been identified. However, detailed molecular mechanisms of autophagic process have not yet been elucidated. This study uncovered a novel role of cathepsin B (CTSB), a lysosomal protease, in autolysosome clearance, termed autolysosome efflux. CTSB-deficient immortalized and primary macrophages showed higher accumulations of autophagy specific protein microtubule-associated protein 1 light chain 3(LC3)-II and they showed greater numbers of FITC-LC3 punta within the cells. These LC3 punta colocalized with dequenched (DQ)-fluorescent-conjugatedBSA, a lysosomal fluorescent marker, which indicated that the accumulating autophagy vesicles in CTSB-deficient cells were autolysosomes. Further investigations showed that CTSB-deficient macrophages accumulated autolyososomes due to defects in autolysosome efflux. These results suggested that CTSB is a key player in mediating autolysosome efflux. A clear linkage between autolysosome efflux and cell death was not found. This study implicates that CTSB may be used as a potential tool to further investigate autolysosome vesicle trafficking and identify the role of autolysosome efflux. Further research in autolysosome efflux will provide insights into the autophagy life cycle and possibly provide novel therapeutic strategies for treating many diseases caused by defective or overactive autophagy such as neurodegenerative diseases, pancreatitis or cancer.

Keywords

cathepsin B, autophagy, autophagosome, autolysosomes, efflux, macrophages

ACKNOWLEDGEMENTS

I would like to acknowledge my supervisor, Dr. Sung Kim, whose understanding, guidance and support have helped me throughout my years at the University of Western Ontario and during the production of this thesis.

I would also like to thank my committee members Dr. Barr and Dr. Mymryk for their encouragements and insightful suggestions throughout my thesis project.

Many thanks to everyone (past and present) in the Kim lab and especially Dr. Soon D. Ha and Andrew Martins who provided me with help and advice whenever I needed them.

And I would like to thank members of the McCormick lab for all the help they provided me.

TABLE OF CONTENTS

TITLE PAGE i
CERTIFICATE EXAMINATION ii
ABSTRACT iii
ACKNOWLEDGEMENTS iv
TABLE OF CONTENTS v
LIST OF FIGURES vii
ABBREVIATIONS viii

CHAPTER 1- INTRODUCTION 1
1.1. AUTOPHAGY 1
1.2. MOLECULAR MECHANISM OF AUTOPHAGIC PATHWAY 2
1.2.1. Formation of autophagosomes 2
1.2.2. Maturation of autophagosomes 8
1.3. BIOLOGICAL FUNCTION OF AUTOPHAGY 10
1.3.1. Autophagy and cell survival 10
1.3.2. Autophagy and cell death 10
1.4. CATHEPSIN B 13
1.4.1. CTSB and cell death 13
1.4.2. CTSB and vesicle trafficking 14
1.5. RATIONALE, HYPOTHESIS AND OBJECTIVES 15

CHAPTER 2 – MATERIALS AND METHODS 16
2.1. MATERIALS AND REAGENTS 16
2.2. CELL CULTURE 16
2.3. PREPARATION OF MOUSE PERITONEAL MACROPHAGE 16
2.4. TOTAL CELL LYSATE PREPARATION AND IMMUNOBLOT ANALYSIS 17
2.5. AUTOLYSOSOME EFFLUX ANALYSIS 17
2.6. STATISTICAL ANALYSIS 18
2.7. MEASUREMENT OF CELL VIABILITY 19
2.7.1. CELL VIABILITY ASSAY 19
2.7.2. MTT ASSAY 19

CHAPTER 3 – RESULTS 20
3.1. CTSB IS INVOLVED IN AUTOLYSOSOME EFFLUX 20
3.1.1. CTSB-deficient macrophages show higher acidic vacuole accumulation 20
3.1.2. CTSB deficient macrophages show higher accumulation of autophagic vesicles 20
3.1.3. Autolysosome efflux is defective in CTSB-deficient macrophages 28
3.2. FUNCTION OF AUTOLYSOSOME EFFLUX 36
3.2.1. Autolysosome efflux and autophagy-induced cell death 36

CHAPTER 4 – DISCUSSION 54
4.1. CTSB-mediated autlysosome efflux 54
4.1.1. Limitations 60
4.2. Physiological role of autolysosome efflux 61
4.2.1. LPS + zVAD induced cell death 61
4.2.2. LeTx induced cell death 63
4.2.3. Serum starvation induced cell death 64

4.2.4. CTSB-mediated autolysome efflux is required for anthrax toxin receptor 2-mediated anthrax toxin delivery into the cytoplasm. 64
4.3. Future directions 65
4.3.1. CTSB protease activity and autolysosome efflux 66
4.3.2. Potential proteases involved in autolysosome efflux 66
4.3.3. Potential proteins involved in autolysosome efflux 67
4.4. Conclusion 68

APPENDIX 69
REFERENCES 75
VITA 82

LIST OF FIGURES

Figure	Description	Page
1.1	A schematic diagrame of the autophagic pathways	3
1.2	A schematic diagram of the two ubiquitin-like conjugation pathways required for IM elongation	6
3.1	CTSB-deficient BMDIM accumulates acidic vacuoles	21
3.2	CTSB-deficient BMDIM accumulates LC3-II.	24
3.3	CTSB-deficient primary peritoneal macrophages have higher LC3-II accumulation.	26
3.4	CTSB-deficient BMDIM show higher amount of autophagic vesicles.	28
3.5	CTSB-deficient macrophages show higher amount of autophagic vesicles.	31
3.6	CTSB-deficient BMDIM have defect in autolysosome efflux.	33
3.7	CTSB-deficient peritoneal macrophages have a defect in autolysosome efflux.	37
3.8	CTSB inhibition shows defect in autolysosome efflux.	39
3.9	CTSB-deficient BMDIM are susceptible to LPS+zVAD-induced cell death	41
3.10	LPS+zVAD induced cell death in $CTSB^{+/+}$ and $CTSB^{-/-}$ macrophages.	44
3.11	CTSB-deficient BMDIM are susceptible to LeTx-induced cell death.	47
3.12	CTSB-deficient peritoneal macrophages are sensitized to LeTx induced cell death	49
3.13	CTSB-deficient BMDIM are not sensitized to serum starvation-induced cell death.	52
4.1	A diagram illustrating involvement of CTSB in vesicle trafficking.	57
Appx A1	MG132 inhibits LeTx induced cell death in CTSB-deficient BMDIM	70
Appx A2	3-MA treatment induces LC3-II.	72

ABBREVIATIONS

3-MA	3-methyl adenine
ATG	autophagy related
Aβ	amyloid-β peptide
BMDIM	bone marrow-derived immortalized macrophages
CTSB	cathepsin B
DMSO	Dimethyl sulfoxide
DQ-BSA	dequenched (DQ)-green fluorescent-conjugates of bovine serum albumin (BSA)
EBNA1	Epstein-Barr virus nuclear antigen 1
IM	isolation membrane
LAMP	lysosomal associated membrane proteins
LC3	microtubule-associated protein 1 light chain 3
LeTx	anthrax lethal toxin
LF	lethal factor
LPS	lipopolysaccharide
MHC	major histocompatibility complex
MTT	3-(4,5-Dimethylthiazol-2-yl)-2,5-diphenyltetrazolium bromide, a tetrazole
MVBs	multivesicular bodies
NALP1b	NACHT-leucine-rich repeat and pyrin domain-containing protein 1b
Nec-1	Necrostatin 1

NLR	nucleotide-binding domain-, leucine-rich repeat (LRR)-containing receptor
NPC	Niemann-Pick C
PA	protective antigen
PCD	programmed cell death
PE	Phosphatidylethanolamine
PI	propidium iodide
PI3K	phosphoinositide kinase-3
PtdINs	phosphatidylinositols
Q-SNAREs	glutamine-containing SNAREs
RIP-1	receptor interacting protein -1
ROS	reactive oxygen species
R-SNAREs	arginine-containing SNAREs
SDS-PAGE	sodium dodecyl sulfate polyacrylamide gel electrophoresis
SNAP-25	25 kDa synaptosome-associated protein
SNARE	soluble NSF attachment protein receptor where NSF stands for *N*-ethyl-maleimide-sensitive fusion protein
SPARC	secreted protein, acidic and rich in cysteine
TNF	tumor necrosis factor
VAMP	vesicle associated membrane protein
Vti1b	Vesicle transport through interaction with t-SNAREs homolog 1b
zVAD	benzyloxycarbonyl-Val-Ala-Asp

Chapter 1 -Introduction

1.1. Autophagy

Autophagy is a vesicular system which functions as a lysosomal degradation pathway found in organisms ranging from yeast to mammals[1]. To date three types of autophagy have been characterized based on their physiological functions and modes of formation: chaperone-mediated autophagy, microautophagy and macroautophagy. In chaperone mediated autophagy, specific proteins are transported into lysosomes with the help of chaperone proteins[2]. Micro- and macroautophagy involve cytoplasmic sequestration by vesicles, followed by the delivery of vesicles to lysosomes for the degradation and recycling of vesicle contents[3]. Macroautophagy involves the formation of a cytosolic double membrane vesicle that fuses with the lysosome. In contrast, microautophagy involves sequestration of the cytosol or whole organelles at the surface of the degradative organelle and it doesn't require intermediate transport vesicles[4]. The focus of this thesis will be on macroautophagy which will be referred to as autophagy from this point on.

In normal conditions, autophagy is an important process in maintaining cellular homeostasis by degrading damaged organelles and proteins as energy sources[1]. Autophagy is also an important stress adaptation mechanism during hypoxia, nutrient deprivation and growth factor depletion[5-6]. In the immune system, autophagy plays important roles in innate immunity, such as limiting viral replication[7], facilitating bacterial degradation[8-9] and providing protection against bacterial toxins[10]. In addition, autophagy is an important component of adaptive immunity as it is involved in Major Histocompatibility Complex (MHC) class II antigen presentation by processing long-lived endogenous proteins[11]. Thus, autophagy is an essential process in both cell survival and immune defense systems. Defects in autophagy can lead to several diseases such as pancreatitis[12], neurodegenerative diseases[13] and cancer[14]. At the same

time, uncontrolled autophagy has been reported to be involved in cell death. For example, macrophages and fibroblasts exhibited accumulations of autophagic vesicles upon certain cell death stimuli, which were prevented by inhibiting the autophagy process[15-18]. The mechanism by which autophagy may contribute to cell death remains unknown and further investigations are required to elucidate the roles of autophagy in cell death[1, 5, 19].

1.2. Molecular mechanism of autophagy pathways

1.2.1. Formation of autophagosomes

Autophagy is a dynamic multistep process which requires multiple gene products, referred to as ATG proteins[5]. Autophagy is initiated by the formation of a cup-shaped structured membrane, called isolation membrane (IM; also known as phagophore) within the cytosol (Figure 1.1). The IM elongates and encloses cytosolic components within a double membrane vesicle, known as autophagosome. Initiation of autophagy is mediated by the formation of ATG 1, ATG 17 and ATG 13 complex, which is negatively regulated by the serine/theronine kinase mTOR[20]. In normal conditions, constitutively activated mTOR phosphorylates ATG 13 and prevents the ATG 1/ATG 13 complex formation. During nutrient deprivation, mTOR is inhibited and ATG 13 is dephosphorylated. Dephosphorlyated ATG 13 then binds to ATG 1 and ATG 17 to initiate autophagy[21].

Another important component involved in the formation of autophagy is a class III phosphoinositide kinase-3 (PI3K) complex that consists of Vps34 (a PI3K), beclin-1, ATG 14, and Vps15 (a myristylated kinase)[22]. The PI3K complex is essential for phosphorylation of phosphatidylinositols (PtdINs) to produce phosphatidylinositol 3-phosphates (PtdIns(3)P) which

Figure 1.1. A schematic diagram of the autophagic pathway. Elongation of phagophore/IM forms a double membrane autophagosome. Autophagosomes undergo maturation by fusion with lysosomes to create autolysosomes. Autophagosomes can fuse with early endosome or MVB to form an amphisome which later will fuse with a lysosome to form an autolysosome. In the autolysosomes, the inner membrane as well as the luminal content of the autophagic vacuoles is degraded by lysosomal enzymes that act optimally within this acidic compartment.

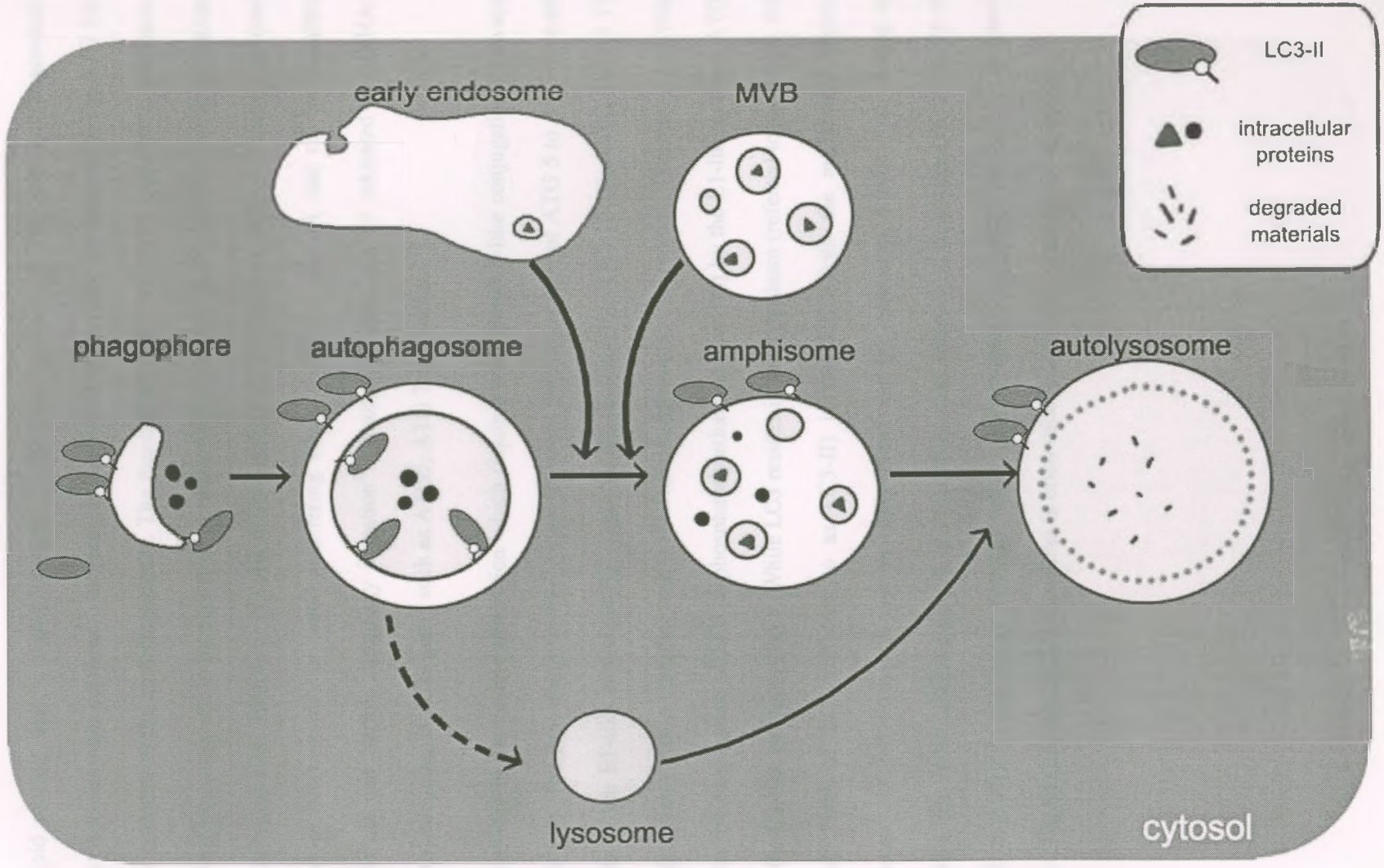
LC3-II
intracellular proteins
degraded materials
early endosome
MVB
phagophore
autophagosome
amphisome
autolysosome
lysosome
cytosol

is a lipid product that is highly enriched in the inner surface of IMs and autophagosomes compared to the outer surfaces[23]. In yeast, PtdIns(3)P is responsible for binding of the ATG 18-ATG 2 complex to the autophagosomes. The function of ATG 18-ATG 2 complex is unknown, but it has been proposed to interact with an unknown component on the IM to promote formation of autophagosomes. Treatment of cells with chemical PI3K inhibitors such as 3-methyl adenine (3-MA) or wortmannin, or small interfering RNAs (siRNAs) against one of the complex components can inhibit autophagy initiation[24]. Autophagy also can be inhibited by siRNA-mediated silencing of ATG genes such as ATG5, ATG 7 and beclin-1[25].

The next step is the vesicle elongation which requires two ubiquitin-like conjugation pathways (Figure 1.2). The first ubiquitin-like system involves the conjugation of ATG 5 to ATG 12 with the help of the E1-like enzyme ATG 7 and the E2-like enzyme ATG 10. The ATG 5-ATG 12 conjugate then forms a complex with ATG 16, called the ATG 16-complex. The second pathway involves the conjugation of LC3 to phosphatidylethanolamine (PE) by the E1-like enzyme ATG 7 and the E2-like enzyme ATG 3. While LC3 resides in the cytoplasm (referred to as LC3-I), the lipidated form of LC3 (referred to as LC3-II) is associated with the autophagic vesicle membrane. LC3-II formation can be easily monitored by examining a shift from diffuse to punctuate fluorescent staining pattern of the protein or an increase of electrophoretic mobility of LC3-II on SDS-PAGE (sodium dodecyl sulfate polyacrylamide gel electrophoresis) compared with LC3-I. Examining LC3-II formation is often used to detect the presence of autophagy [25].

Figure 1.2 A schematic diagram of the two ubiquitin-like conjugation pathways required for IM elongation (adapted from [26]). ATG 12 is activated by ATG 7 (an E1 enzyme), transferred to ATG 10 (an E2 enzyme) and conjugated to ATG 5 which later forms a complex with ATG 16, called ATG 16L complex. The second modifier necessary for autophagosome formation is LC3, a cytosolic form LC3-I is activated by ATG 7, transferred to ATG 3 (an E2 enzyme) and finally conjugated with phosphatidylethanolamine (PE), generating the membrane bound form LC3-II.

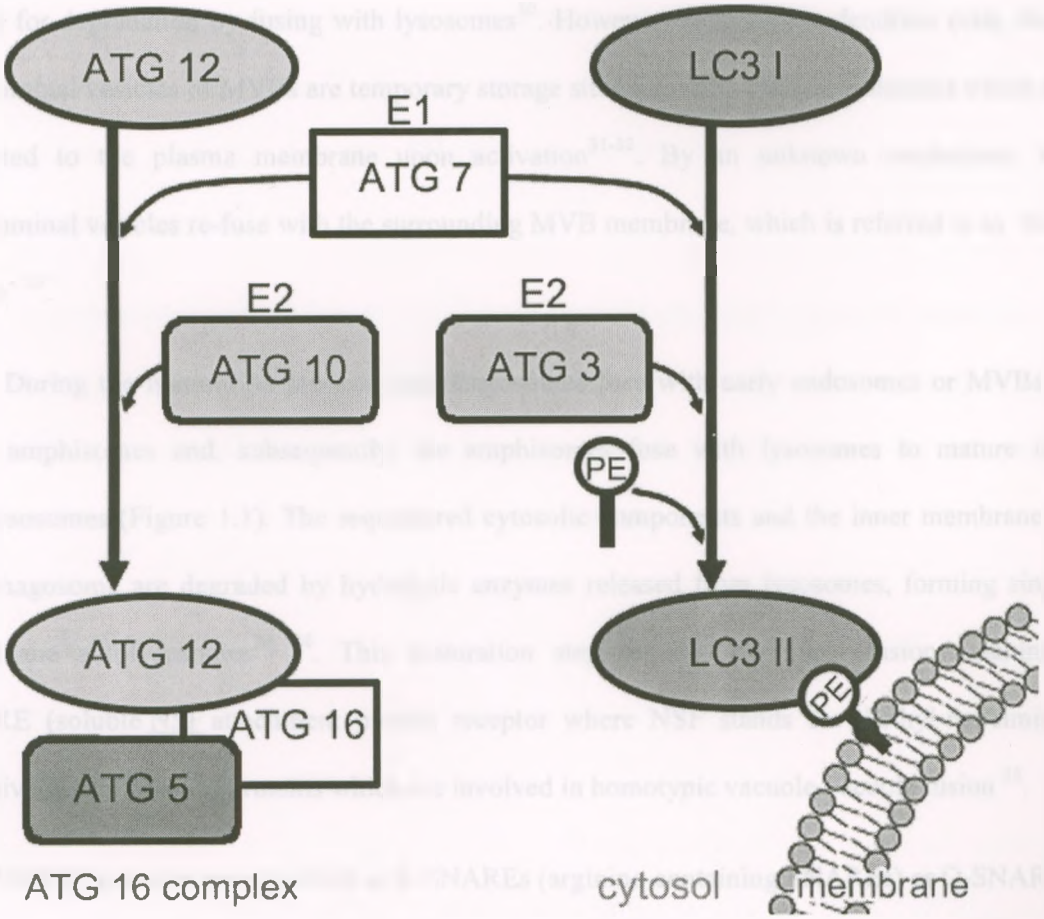
ATG 12
LC3 I
E1
ATG 7
E2
ATG 10
E2
ATG 3
PE
ATG 12
ATG 16
ATG 5
LC3 II
PE
ATG 16 complex
cytosol
membrane

syntaxin, vesicle associated membrane protein (VAMP, also called synaptobrevin[37]) or 25 kDa synaptosome-associated protein (SNAP-25) families[38]. Sets of SNARE proteins are involved in membrane fusion by assembling into core complexes[39]. On membranes, SNARE proteins have been found to be localized to cholesterol-rich lipid-raft membrane domains[40].

Regarding autophagy vesicle trafficking, SNARE proteins have been identified to be involved in autophagosome maturation. In *Saccharomyces cerevisiae*, SNARE proteins such as Sec18 (NSF) and Vesicle transport through interaction with t-SNAREs homolog 1b (Vti1b; a SNARE), which are generally involved in homotypic vesicle fusions, are also required for autophagosome vacuole fusion[41]. In mammalian cells, Vti1b knockout mice accumulate autophagosomes, showing that this SNARE and its SNARE complex are required for autolysosome maturation[42].

Once autolysosomes are formed, the degraded protein products or degraded organelles are released into the cytosol or extracellular space[43]. To date, information regarding the mechanism of autolysosome degradation or its clearance is limited. In this thesis, the process of autolysosome clearance will be termed 'autolysosome efflux'.

1.3. Biological function of autophagy

1.3.1. Autophagy and cell survival

Autophagy is a cellular process required for the proper degradation of proteins and this important function of autophagy is apparent during nutrient deprivation. In yeast, autophagy provides energy by breaking down proteins[44]. Established cancer cells utilize autophagy for cell survival during starvation and hypoxia[14]. Autophagy is also essential for maintaining cellular fitness. Genetic knockdown of ATG 7 or ATG 5 in mice induces accumulation of ubiquitinated proteins[45] or neuro-degeneration, respectively[46]. Neurons in Alzheimer's disease show impaired maturation of autophagosomes to autolysosomes which results in an accumulation of amyloid-β peptide (Aβ), a key pathogenic factor of Alzheimer's disease, within autophagosomes[13, 47]. Defects in autophagy lead to DNA damage[14, 48], protein aggregation[49], and generation of reactive oxygen species (ROS)[50] which can lead to cancer. Thus, autophagy is critical for the maintenance of cellular protein and organelle homeostasis and, during stress, it is an essential cell survival mechanism which provides extra sources of nutrients and energy.

1.3.2. Autophagy and cell death

Despite its role in cell survival, autophagy is associated with certain cell death. There are at least three different cell death programs described: apoptotic cell death, which is the most extensively studied cell death, necrotic cell death[51-53] and autophagic cell death[52-53]. Apoptosis is characterized by distinct morphological features including cell shrinkage, membrane blebbing, chromatin condensation, nuclear fragmentation and budding off of apoptotic bodies[54]. Apoptosis is initiated by serial activation of various cysteine-aspartyl-specific proteases (caspases) including caspases-2,-3,-6,-7,-8,-9 and -10[54-57]. Apoptosis also involves the release of

cytochrome c from the mitochondria through the outer membrane pores composed of pro-apoptotic mitochondrial proteins such as BID[58] and BAX[59].

Necrosis is morphologically described by cytoplasmic swelling, rupturing of the plasma membrane, and nuclear fragmentation. In contrast to apoptosis, necrotic cell death causes inflammation as it can lead to release of pro-inflammatory cytokines such as IL-8, and TNF-α[60]. The molecular mechanisms of necrosis are still poorly understood[61]. Intracellular events that are commonly observed in necrotic cell death are the production of reactive oxygen species (ROS) by mitochondria, release of lysosomal proteases such as calpains and cathepsins into the cytoplasm, and failure of Ca^{2+} homeostasis[61].

Autophagic cell death is morphologically characterized as cell death in the presence of autophagy[62]. Autophagic cell death has been observed during the development of diverse organisms[63-65] and different cell types such as macrophages[16], acinar cells[66] and neuronal cells[62]. The molecular mechanism of autophagic cell death is considered to be caspase-independent[16-18]. However, autophagy has been shown to be involved in caspase-dependent cell death[64, 67]. Therefore, a clear mechanism of autophagic cell death still remains to be defined.

As previously mentioned, autophagic cell death is usually described to be a caspase-independent process and this has been demonstrated in macrophages and fibroblasts[16-18]. In macrophages, caspase-independent autophagic cell death has been demonstrated with bacterial lipopolysaccharides (LPS) and pan-caspase inhibitor benzyloxycarbonyl-Val-Ala-Asp (zVAD) treatment[16]. Treatment with LPS alone increases apoptotic events such as caspase-8 and DNA fragmentation[68-69]. In addition, it also cleaves receptor interacting protein-1 (RIP-1) which is upstream of ROS production[16, 70]. When macrophages are treated with zVAD in addition to LPS, they show a greater degree of cell death[16]. Macrophages undergoing LPS and zVAD-induced cell

death show an accumulation of autophagic vesicles and ROS production. Treatment with 3-MA or treatment with siRNAs against beclin-1 prevents LPS and zVAD-treatment induced cell death, which indicates that autophagy is required for this process.

Yu *et al.*, showed treatment of L929 fibroblast cells with zVAD induces autophagy-dependent cell death which is downstream of RIP-1 activation[18]. They demonstrated that autophagy is responsible for inducing cell death, because treating the cells with ATG 7 or beclin-1 siRNA prevented cell death. Interestingly, they showed a correlation between zVAD-induced cell death and ROS accumulation, both of which are inhibited by treating the cells with the PI3K inhibitor wortmannin[17].

Physiologically, autophagy has been reported to play a role in caspase-dependent cell death in salivary gland cells during *Drosophila* development. It was shown that there is an increase in caspase transcription levels, increased caspase activity, and DNA fragmentation, which are characteristics of apoptosis. Yet there is also accumulation of vacuolar structures that resemble autophagic vesicles[71], and ATG7 knockdown results in incomplete degradation of salivary gland during *Drosophila* development *in vivo*[72]. In medulla blastomas, autophagy also has been reported to be involved in caspase-dependent cell death[67]. Treatment with the matrix-associated glycoprotein secreted protein, acidic and rich in cysteine (SPARC) induces autophagy, which is upstream of caspase-3 and caspase-8 activation. Autophagy inhibition by 3-MA blocks caspase activation and caspase-dependent apoptotic cell death.

1.4. Cathepsin B

Cathepsin B (CTSB) is a lysosomal cysteine protease of the papain family that has exopeptidase activity at acidic pH (4-5) and endopeptidase function at neutral pH[73]. CTSB is ubiquitiously expressed in many different cell types[74]. It is localized in the lysosome, but also found in the cytoplasm[75] and the periplasmic space[76]. Cytosolic localization of CTSB is important for cell death such as apoptosis as it is involved in caspase-3 activation[75]. CTSB has also been shown to be involved in the activation of the NOD-like receptor family, pryin domain containing 3 (NLRP3), which induces caspase-1 activation and the secretion of proinflammatory cytokines including interleukin-1β, 18 and 23[77]. In the periplasmic space, CTSB is involved in extracellular matrix remodeling[73] by degrading extracellular matrix proteins such as laminin, fibronectin and collagen IV at both neutral and acidic pHs[78-79]. CTSB can also activate other proteolytic enzymes such as latent collagenase which is capable of digesting fibrillar collagen in extracellular matrix[80-81]. Hence, CTSB has been reported to be important for cancer metastasis[73] and its expression is often increased specifically at the invasive edge of tumors[82].

1.4.1. Cathepsin B and cell death

CTSB has been shown to be involved in apoptosis. Apoptosis induced by overexpression of p53 or cytotoxic agents can be blocked by pharmacological inhibition of CTSB[83]. Other studies revealed that CTSB is released into the cytosol and causes cytochrome c release from mitochondria[84], resulting in the activation of caspase-3 and, ultimately, cell death[67, 85]. CTSB has also been shown to be involved in non-apoptotic cell death. For example, PC12, a rat pheochromocytoma cell line, undergoes a caspase- and autophagy-dependent cell death in the absence of the nerve growth factor[62]. Interestingly, the cell death is prevented by caspase-3

inhibition alone; however, when caspase-3 and CTSB are inhibited together, the cells are no longer protected from death[62]. This study indicated that CTSB may play a protective role in caspase-independent cell death, given that the caspase-dependent cell death process was prevented by a caspase-3 inhibitor. Hence, it is possible that autophagy-dependent cell death could have proceeded in the presence of a CTSB inhibitor; however, more specific and detailed experiments are required to determine whether CTSB is involved in autophagy-dependent cell death.

1.4.2. Cathepsin B and vesicle trafficking

In previous studies, lysosomal proteases have been suggested to be involved in lysosomal vacuole trafficking. In yeast, inhibition of a lysosomal protease, proteinase B, caused accumulation of autophagic vacuoles[86]. In cathepsin B and L knockout mice, neuronal tissues shows large vacuole accumulations[87]. Our previous study showed that CTSB is required for the transportation of TNF-α containing vesicles to the plasma membrane in macrophages[88]. Rat pancreatic acinar cells treated with CA-074ME, a cathepsin B inhibitor, show accumulation of large vacuoles which contain partially degraded materials. In pancreatitis, acinar cells have defective maturation of CTSB[89], resulting in the accumulation of vesicles that are positive for lysosomal and autophagic markers, lysosomal associated membrane proteins (LAMP)-2 and LC3-II, respectively[12]. These observations suggest that CTSB plays a crucial role in vesicle or lysosomal vacuole trafficking.

1.5. Rationale, Hypothesis and Research Objectives

CTSB is a lysosomal protease that is involved in matrix remodeling, vesicle trafficking and cell death. CTSB has also been reported to play a protective role in caspase-independent cell death, and its absence can lead to cell death. Hence, these data suggests that CTSB may play a protective role in autophagic cell death by maintaining proper vesicle trafficking, possibly after the formation of autolysosomes. Therefore, I hypothesize that CTSB is required for autolysosome clearance (efflux), and that inhibition of autolysosome efflux causes autophagic cell death. In order to address this hypothesis, I first assessed if CTSB is important for autophagy vesicle trafficking using macrophages from mice with genetic knockdown of CTSB and, if so, at which step of autophagy CTSB plays a role. I then investigated whether a defect in autophagy efflux sensitizes cells to autophagy cell death using three different autophagic cell death inducing stimuli: anthrax lethal toxin, LPS+zVAD and serum starvation.

Chapter 2 - Methods and Materials

2.1. Materials and Reagents

CTSB inhibitor IV (CA074-Me) was purchased from Peptide Institute (Osaka, Japan). MG132 were purchased from Calbiochem. LF and PA were prepared in the laboratory as previously described [90-91]. Antibodies for LC3 and p38 mitogen-activated protein kinase were obtained from Cell Signaling Technologies (Pickering, ON). Antibodies for actin were obtained from Abcam (Cambridge, MA).

2.2. Cell Culture

The human monocytic cell line THP-1 and bone marrow-derived immortalized macrophages (BMDIM) from a C57BL/6 mouse (obtained from Dr. B. Aggarwal, Houston, TX) were cultured in RPMI (Roswell Park Memorial Institute)1640 medium containing 10% heat-inactivated fetal bovine serum (Sigma), 10 mM MEM (Modified Eagle's Medium) nonessential amino acids solution, 100 units/ml penicillin G sodium, 100 μg/ml streptomycin sulfate, and 1 mM sodium pyruvate. Cells were grown at 37 °C in a humidified atmosphere containing 5% CO_2.

2.3. Preparation of Mouse Peritoneal macrophages

Resident peritoneal macrophages were obtained from mice by normal saline lavage. Mice received intraperitoneal injection of 3% thioglycollate 4 days before the preparation of peritoneal macrophages. Peritoneal macrophages were harvested by the lavage of the peritoneal cavity with 5 ml of phosphate-buffered saline. Cells were incubated at 37 °C overnight in a humidified atmosphere of 5% CO2.

2.4. Total Cell Lysate Preparation and Immunoblot Analysis

Total cell lysate preparation and immunoblotting procedures were performed as previously described [92]. Briefly, cells were lysed in ice-cold lysis buffer (20 mM MOPS, 2 mM EGTA, 5 mM EDTA, 1 mM Na_3VO_4, 40 mM β-glycerophosphate, 30 mM sodium fluoride, 20 mM sodium pyrophosphate, and 1% Triton X, pH 7.2) containing a protease inhibitor mixture (Roche Applied Science). The cell lysates were incubated on ice for 10 min and centrifuged at 12,500 rpm for 15 min at 4 °C. The supernatants were separated by SDS-polyacrylamide gels followed by transfer onto nitrocellulose membranes (Bio-Rad). The membranes were blocked with 5% (w/v) skim milk for 1 h at room temperature and then incubated overnight at room temperature with the primary antibody. The membranes were washed, incubated with secondary antibody for 1 h (Pierce), and developed using an enhanced chemiluminescence detection system (ECL) (Pierce).

2.5. Immunofluorescence Staining and Autophagic Flux Analysis

For immunofluorescence staining, macrophages were plated on coverslips and were fixed with 4% formaldehyde. Immunofluorescent staining was performed using anti-LC3 primary antibodies biotinylated anti-rabbit IgG secondary antibodies and TexasRed-avidin D (Vector Laboratories). The stained cells were imaged using an Olympus IX51 microscope and Q Capture Pro 6.0 software. Autophagy flux was analyzed by flow cytometry and fluorescent microscopy using DQ™ Red BSA (self-quenched red BODIPY dye conjugated to BSA; Molecular Probes, Eugene, OR) and DQ™ Green BSA. DQ-BSA requires enzymatic cleavage in acidic intracellular lysosomal compartments to generate a highly fluorescent product that can be monitored by fluorescent microscopy or flow cytometry. BMDIM were incubated in RPMI

media containing DQ-BSA® Green (10 µg/ml) for 15 min and washed twice with PBS. Cells were then further incubated in media for 6H and the cells were fixed with 4% formaldehyde. Immunofluorescent staining was performed using anti-LC3 primary antibodies biotinylated anti-rabbit IgG secondary antibodies and TexasRed-avidin D. Colocalizations of TexasRed-LC3 and red fluorescent of DQ-BSA were imaged using an Olympus IX51 microscope and Q Capture Pro 6.0 software. For flow cytometry analysis, the human monocytic cell line THP-1 was incubated in RPMI media containing DQ-BSA (10 µg/ml) for 15 min at 37 °C in 5% CO_2. Cells were washed twice with PBS and then incubated for 45 min to ensure that DQ-BSA had reached the lysosomal compartment. THP-1 cells were further incubated in the presence or absence of CA074-Me for the indicated times. Cells were harvested, and red-fluorescence of DQ-BSA was analyzed by flow cytometry using a FACSCalibur flow cytometer (BD Biosciences), and CellQuest (BD Biosciences) and FlowJo (Treestar) v. 7.2.4 software. For confocal images analysis, cells were plated on coverslips after treatment as above and fixed with 4% formaldehyde. The fluorescent degradation products of DQ-BSA in lysosomes were imaged using a Bio-Rad Radiance 2000 two-photon confocal microscope and LaserSharp 2000 software.

2.6. Statistical analyses

Statistical significance was determined by unpaired Student's t-test using a GraphPad Prism v.5. Differences were considered significant with a P-value <0.05.

2.7. Measurement of Cell Viability

2.7.1. Cell Viability Assay

The extent of cell death was measured using either crystal violet uptake in live cells or propidium iodide (PI; Sigma, Irvine, CA) permeability analysis. The crystal violet uptake assays were performed as described previously [93]. The integrity of the plasma membrane was assessed by determining the ability of cells to exclude PI. Cells were trypsinized, collected by centrifugation, washed once with PBS, and resuspended in PBS containing 1 μg/ml PI. The levels of PI incorporation were quantified by CellQuest software on a FACSCalibur flow cytometer (Becton Dickinson). Cell size was evaluated by forward-angle light scattering. PI-negative cells were considered to be live cells.

2.7.2. MTT Assay

MTT assays were performed in a 96-well plate according to manufacturer's instruction (Sigma). Briefly, after treatment, MTT was added to each well at a final concentration of 250 μg/ml. After incubating at 37 °C for an additional 2 h, culture media was carefully aspirated, and 100 μl of dimethyl sulfoxide (DMSO) was added to dissolve crystals. Optical densities of the wells were analyzed using an automatic enzyme-linked immunosorbent assay plate reader (Bio-Rad) at a wavelength of 590 nm. The ratio of cell death was determined based on the optical density of the treated wells compared with those from nontreated cells with no cell death.

Chapter 3-Results

3.1. CTSB is involved in autolysosome efflux

3.1.1. CTSB-deficient macrophages accumulate larger acidic vacuoles than wild type macrophages.

To examine whether CTSB is involved in vacuole trafficking, bone marrow-derived immortalized macrophages (BMDIM) prepared from C57BL6/j ($CTSB^{+/+}$) or $CTSB^{-/-}$ (C57BL6/j background) mice were examined under a microscope. Large vacuoles were readily detected in non-treated $CTSB^{-/-}$ but not in $CTSB^{+/+}$ BMDIM (Figure 3.1, row 1). When cells were exposed to various known autophagy inducing agents including LPS (1uM)+zVAD (50uM) or anthrax lethal toxin (LeTx; lethal factor (LF) 250 ng/ml and protective antigen (PA) 1500 ng/mL), or were cultured in serum-deprived media (Serum Starvation), the sizes of these vacuoles were further increased in $CTSB^{-/-}$ cells (Figure 3.1, rows 2-4). These vacuoles were co-localized with red fluorescent puncta in cells treated with LysoTracker® Red, a membrane permeable red fluorescent dye that emanates red fluorescence under acidic conditions, suggesting that they are acidic vacuoles. Interestingly, $CTSB^{+/+}$ BMDIM were about 23 μm in diameter, however, not all but many of the $CTSB^{-/-}$ BMDIM were larger than that of $CTSB^{+/+}$ BMDIM (Figure 3.1).

3.1.2. CTSB-deficient macrophages accumulate autophagic vesicles.

LC3-I (18 kDa) converts to a phosphatidylethanolamine-conjugated LC3-II (16 kDa) upon autophagy induction, and the amount of LC3-II in a cell correlates with the extent of autophagic vesicle formation [25]. Large acidic vacuoles were more easily observed in $CTSB^{-/-}$ macrophages than $CTSB^{+/+}$ macrophages. Since even larger acidic vacuoles were viewed in $CTSB^{-/-}$ macrophages treated with autophagy-inducing stimuli, we examined

Figure 3.1. CTSB-deficient BMDIM accumulates acidic vacuoles. BMDIM from C57BL/6j wild type ($CTSB^{+/+}$) and CTSB-deficient ($CTSB^{-/-}$) mice were plated on cover slips. Cells were treated with either LPS (1ug/ml)+zVAD (50uM) for 4 H or LeTx (LF 250 ng/ml and PA 1500 ng/mL) for 3 H, or incubated with cell culture media with (Control (CNT)) or without serum (serum starvation) for 5H. BMDIM were then treated with LysoTracker ® Red for 15 mins and washed with PBS twice. After washing, cells were fixed with 4% formaldehyde and visualized using Olympus fluorescent microscope. [Scale bar: 23μM]. Data represent one of two experiments.

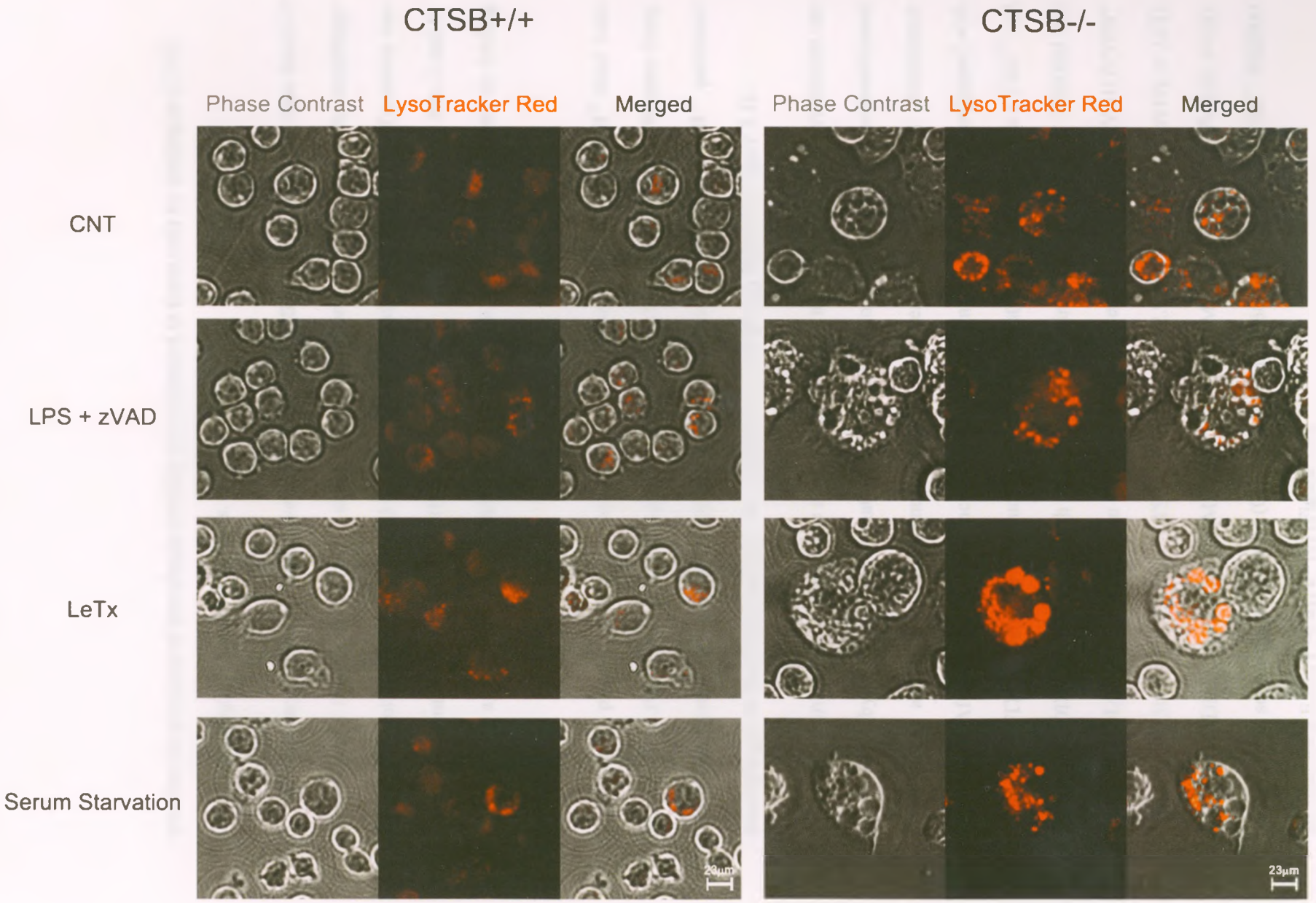
CTSB+/+
CTSB-/-
Phase Contrast
LysoTracker Red
Merged
Phase Contrast
LysoTracker Red
Merged
CNT
LPS + zVAD
LeTx
Serum Starvation
23μm
23μm

whether the presence of autophagic vesicles was enhanced in these cells by looking at LC3-II formation using Western blot analysis.

Without any treatment, basal levels of LC3-II in $CTSB^{-/-}$ cells were higher than those of $CTSB^{+/+}$ cells (Figure 3.2A, lane 1 and 4; Figure 3.2B, lane 1 and 3). All of the autophagy-inducing stimuli slightly induced LC3-II formation in wild-type cells, but LC3-II formation was more prominent in $CTSB^{-/-}$ BMDIM (Figure 3.2A, lane 2, 3, 5 and 6; Figure 3.2B, lane 2 and 4). Immunoblots against the mitogen-activated protein kinase p38 (p38) were used as loading controls[88].

Similarly, primary peritoneal macrophages isolated from $CTSB^{+/+}$ and $CTSB^{-/-}$ mice were treated with LPS+zVAD or LeTx, and LC3-II protein levels were analyzed by Western blots. $CTSB^{-/-}$ peritoneal macrophages showed higher LC3-II protein levels than $CTSB^{+/+}$ peritoneal macrophages at basal level and after the treatments of autophagy inducers (Figure 3.3).

LC3 is recruited to the membrane as autophagy vesicles are formed [5] and the recruitment can be visualized by monitoring the formation of LC3 puncta. To further investigate the involvement of CTSB in autophagy, recruitment of LC3 to vacuoles was visualized by fluorescence microscopy. After immunofluorescence staining of cells using an LC3 antibody-conjugated with biotinylated-FITC, levels of FITC fluorescent puncta formation were examined in $CTSB^{+/+}$ and $CTSB^{-/-}$ BMDIM. In agreement with LC3 Western blots in Figure 3.2, $CTSB^{-/-}$ BMDIM had greater FITC-LC3 punta than those in $CTSB^{+/+}$ BMDIM when treated with LPS+zVAD ($CTSB^{-/-}$ BMDIM 35.30±2.18 S.E.M. vs. $CTSB^{+/+}$ BMDIM 25.3±2.95 S.E.M., $P<0.01$, $n=10$) or LeTx ($CTSB^{-/-}$ BMDIM 30.30±2.80 S.E.M. vs. $CTSB^{+/+}$ BMDIM 19.1±1.51 S.E.M., $P<0.01$, $n=10$), or cultured in serum-deprived media ($CTSB^{-/-}$ BMDIM 29.60±2.49 S.E.M. vs. $CTSB^{+/+}$ BMDIM 20.70±1.48 S.E.M., $P<0.01$, $n=10$) (Figure 3.4).

Figure 3.2. CTSB-deficient BMDIM accumulate LC3-II. BMDIM from C57BL/6j ($CTSB^{+/+}$) or CTSB-deficient ($CTSB^{-/-}$) mice were treated with LPS (1ug/ml)+zVAD (50uM) for 2 H or treated with LeTx (LF 250 ng/ml and PA 1500 ng/mL) for 2 H (A), or incubated with cell culture media with (CNT) or without serum (Serum Starved) for 4H (B). LC3-I and II proteins were analyzed by Western blotting. Western blots against p38 were used as loading controls. Densitometric LC3-II/p38 ratios are shown beside the blots. Data represent one of two independent experiments.

A)

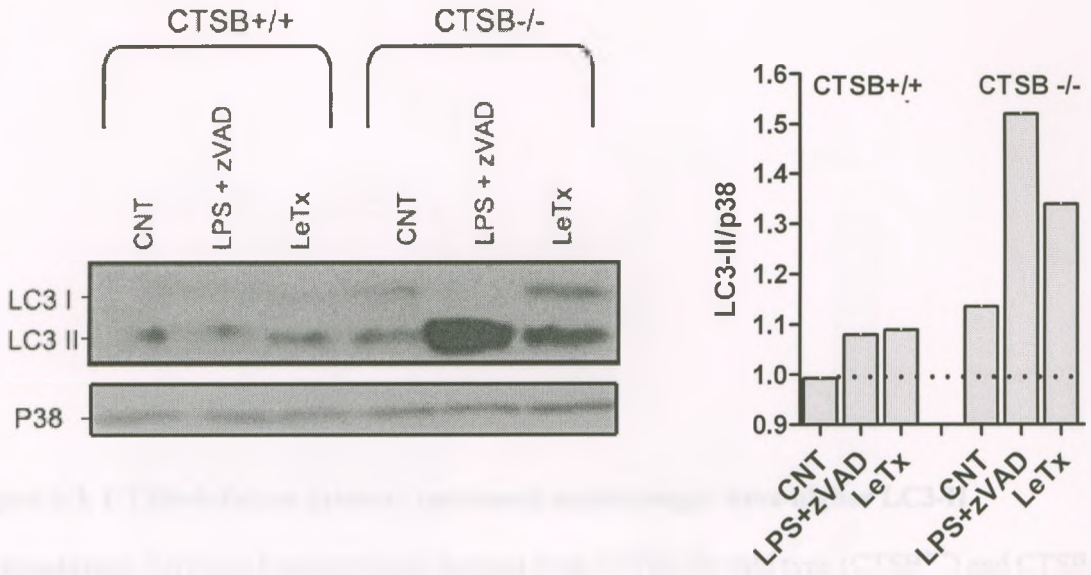
CTSB+/+
CTSB-/-
CNT
LPS + zVAD
LeTx
CNT
LPS + zVAD
LeTx
LC3 I
LC3 II
P38
LC3-II/p38
1.6
1.5
1.4
1.3
1.2
1.1
1.0
0.9
CTSB+/+
CTSB -/-
CNT
LPS+zVAD
LeTx
CNT
LPS+zVAD
LeTx

B)

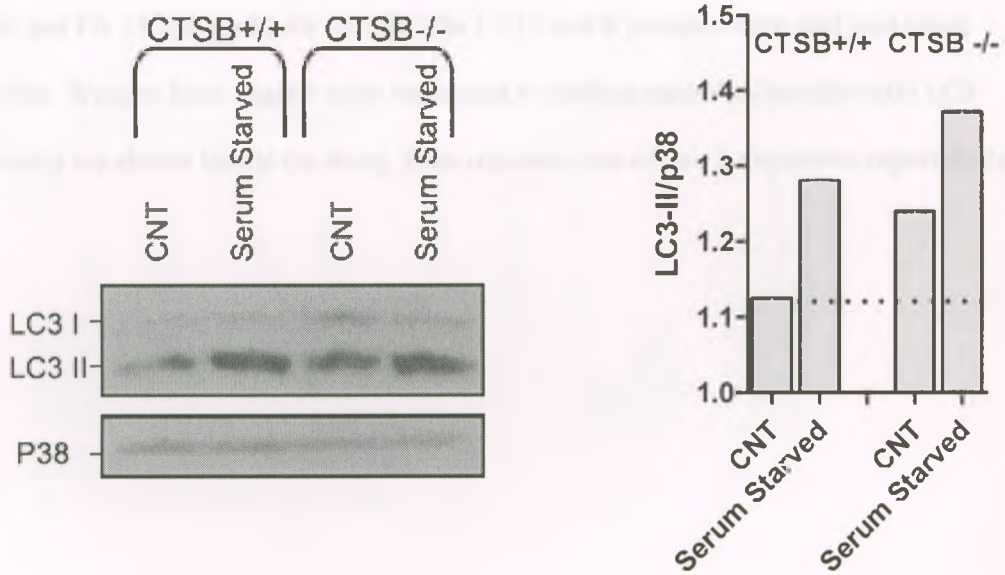
CTSB+/+
CTSB-/-
CNT
Serum Starved
CNT
Serum Starved
LC3 I
LC3 II
P38
LC3-II/p38
1.5
1.4
1.3
1.2
1.1
1.0
CTSB+/+
CTSB -/-
CNT
Serum Starved
CNT
Serum Starved

Figure 3.3. CTSB-deficient primary peritoneal macrophages have higher LC3-II accumulation. Peritoneal macrophages isolated from C57BL/6j wild type ($CTSB^{+/+}$) and CTSB-deficient ($CTSB^{-/-}$) mice were treated with LPS (200ng/ml)+zVAD (50 uM) (A) or LeTx (LF 250 ng/ml and PA 1500 ng/mL) for 2H (B). The LC3 I and II proteins were analyzed using Western blot. Western blots against actin were used as loading controls. Densitometric LC3-II/ratios ratios are shown beside the blots. Data represent one of two independent experiments.

A)

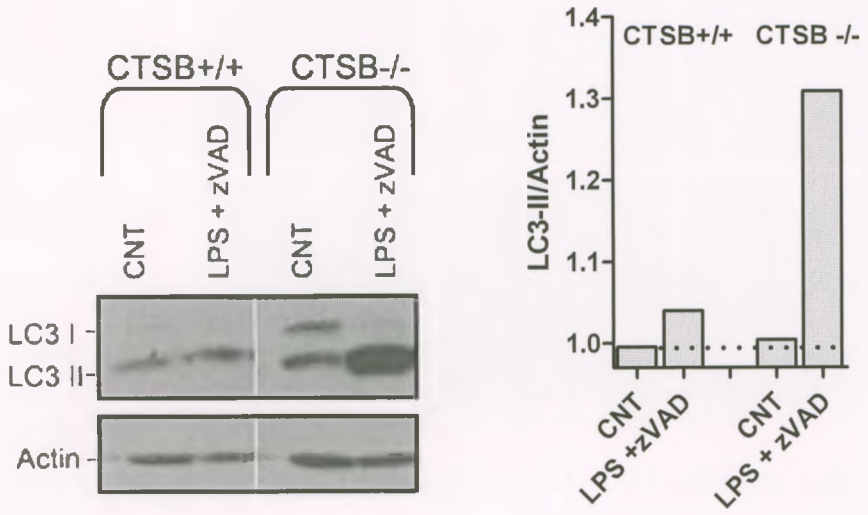
CTSB+/+
CTSB-/-
CNT
LPS + zVAD
CNT
LPS + zVAD
LC3 I
LC3 II
Actin
CTSB+/+ CTSB -/-
LC3-II/Actin
1.4
1.3
1.2
1.1
1.0
CNT
LPS +zVAD
CNT
LPS + zVAD

B)

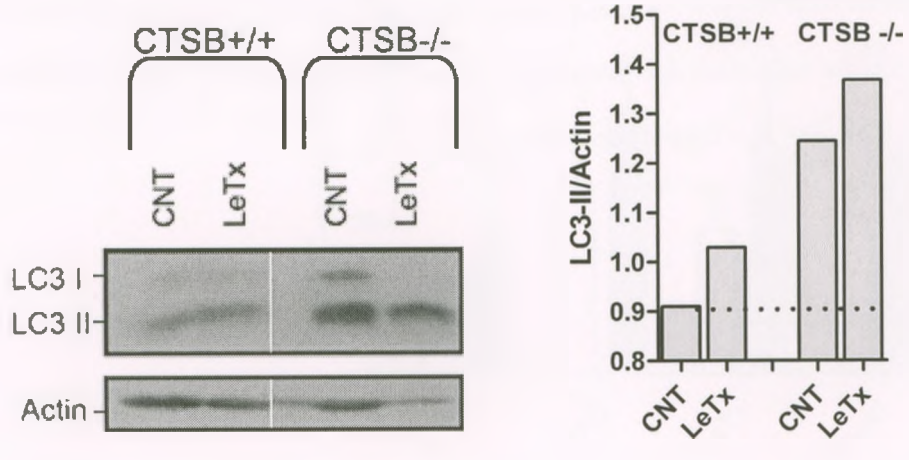
CTSB+/+
CTSB-/-
CNT
LeTx
CNT
LeTx
LC3 I
LC3 II
Actin
CTSB+/+ CTSB -/-
LC3-II/Actin
1.5
1.4
1.3
1.2
1.1
1.0
0.9
0.8
CNT
LeTx
CNT
LeTx

Figure 3.4 CTSB deficient BMDIM show a higher amount of autophagic vesicles.

BMDIM from C57BL/6j ($CTSB^{+/+}$) or CTSB-deficient ($CTSB^{-/-}$) mice were treated with LPS (1ug/ml)+zVAD (50uM) or LeTx(LF 250 ng/ml and PA 1500 ng/mL) for 2 H, or incubated with cell culture media with (CNT) or without serum (Serum Starvation) for 4H. After fixing cells with 4% formaldehyde, immunofluorescent staining was performed using anti-LC3 primary antibodies biotinylated anti-rabbit IgG secondary antibodies and FITC-avidin D. Cells were visualized using an Olympus microscope at 400x magnification (A). [Scale bar: 11μM]. *Dotted lines* indicate the cell margin. Data represents one of two independent trials. LC3-FITC punta per cells were determined (B). Ten cells were counted at random. Mean±S.E.M. **: $P<0.01$. ***: $P < 0.0001$. Student's t-test.

A)

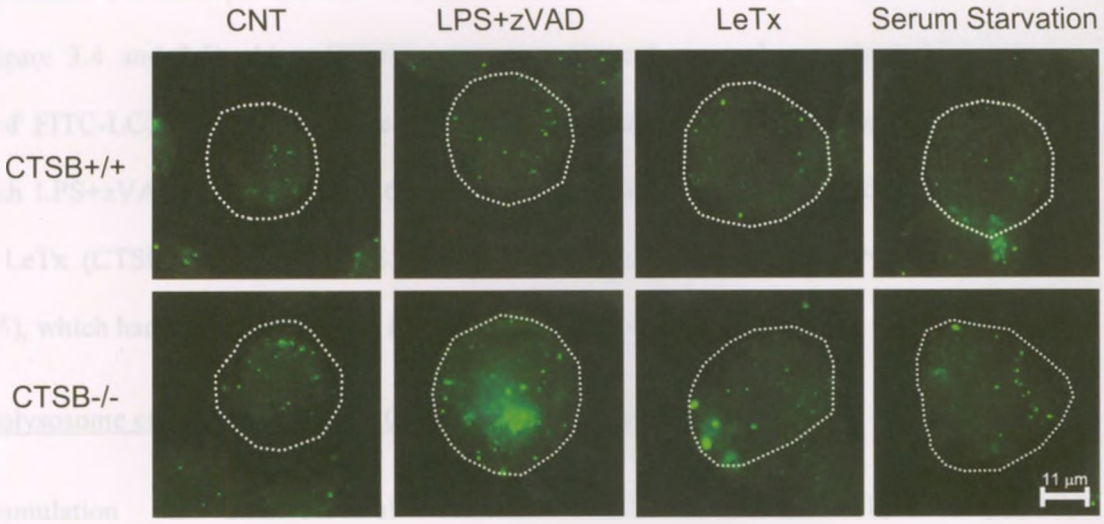

Green = LC3-FITC

B)

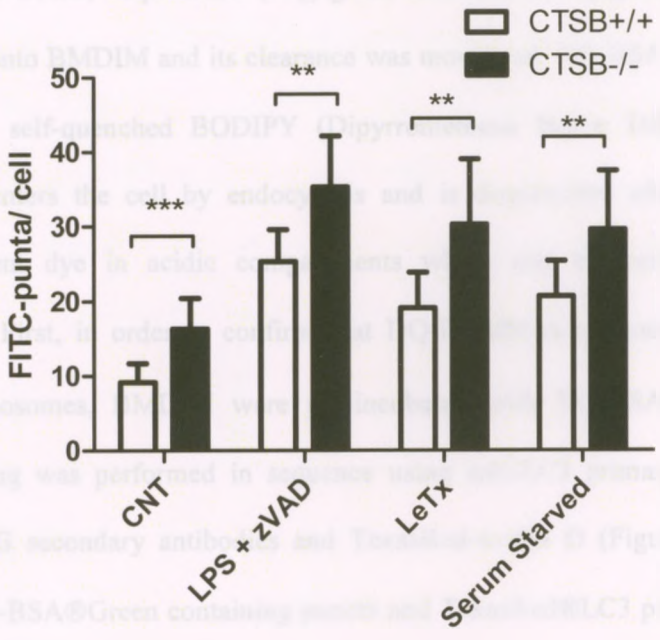

$CTSB^{-/-}$ BMDIM also appeared to have larger FITC-LC3 puncta than those of $CTSB^{+/+}$ BMDIM ($CTSB^{-/-}$ BMDIM 1.04±0.07μm S.E.M. vs. $CTSB^{+/+}$ BMDIM 0.57±0.04μm S.E.M., $P<0.0001$, $n=20$) (Figure 3.4 and 3.5). Also, $CTSB^{-/-}$ primary peritoneal macrophages showed greater numbers of FITC-LC3 puncta than those of $CTSB^{+/+}$ primary peritoneal macrophages when treated with LPS+zVAD ($CTSB^{-/-}$ 56.93±6.95 S.E.M. vs. $CTSB^{+/+}$ 34.27±2.95 S.E.M., $P<0.01$, $n=15$) or LeTx ($CTSB^{-/-}$ 49.20±4.47 S.E.M. vs. $CTSB^{+/+}$ 34.73±3.37 S.E.M., $P<0.05$, $n=15$) (Figure 3.5), which had similar patterns as LC3 Western blots in Figure 3.3.

3.1.3. Autolysosome efflux is defective in CTSB-deficient macrophages.

Accumulation of autolysosomal vesicles could be caused by delayed autophagosome/autolysosome clearance (efflux). To examine whether autolysosome efflux is defective in the absence of CTSB, dequenched (DQ)-green fluorescent-conjugated BSA (DQ-BSA® green) was loaded onto BMDIM and its clearance was monitored. DQ-BSA Green® is a non-membrane permeable self-quenched BODIPY (Dipyrromethene Boron Difluoride) dye conjugated to BSA that enters the cell by endocytosis and is dequenched after enzymatic cleavage of the fluorescent dye in acidic compartments which can be monitored by a fluorescence microscope. First, in order to confirm that DQ-BSA®Green containing puncta were localized to autolysosomes, BMDIM were pre-incubated with DQ-BSA®Green and immunoflurorescent staining was performed in sequence using anti-LC3 primary antibodies, biotinylated anti-rabbit IgG secondary antibodies and TexasRed-avidin D (Figure 3.6A). As shown in Figure 3.6A, DQ-BSA®Green containing puncta and TexasRed®LC3 positive puncta were mostly co-localized (yellow), indicating that DQ-BSA® Green containing vesicles were in fact autolysosomes. Since DQ-BSA® Green positive vesicles were likely autolysosomes, disappearance of DQ-BSA® Green was monitored using fluorescence microscopy.

Figure 3.5. CTSB-deficient primary macrophages show a higher amount of autophagic vesicles. Peritoneal macrophages isolated from C57BL/6j ($CTSB^{+/+}$) or CTSB-deficient ($CTSB^{-/-}$) mice were treated with LPS (200 ng/ml)+zVAD (50uM) or LeTx (LF 250 ng/ml and PA 1500 ng/mL) for 2 H, or incubated with normal media (CNT) . After fixing cells with 4% formaldehyde, immunofluorescent staining was performed using anti-LC3 primary antibodies biotinylated anti-rabbit IgG secondary antibodies and FITC-avidin D. Cells were visualized using Olympus Olympus microscope at 600x magnification (A). [Scale bar: 11μM]. *Dotted lines* indicate the cell margin. Data represents one of two independent trials. LC3-FITC punta per cells were determined (B). Fifteen cells were counted at random. Mean±S.E.M. *P<0.05, **P<0.01. Student's t-test.

A)

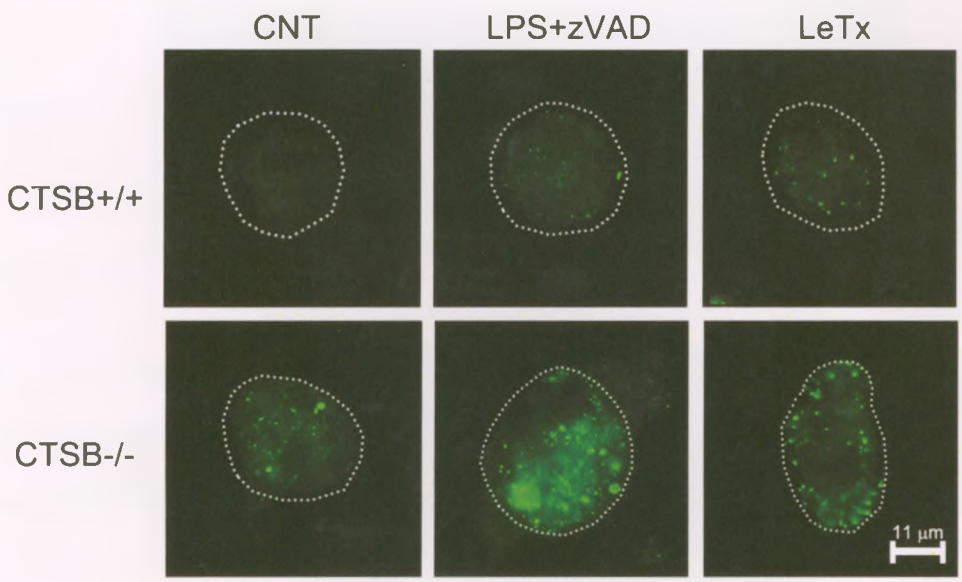

Green= LC3-FIT

B)

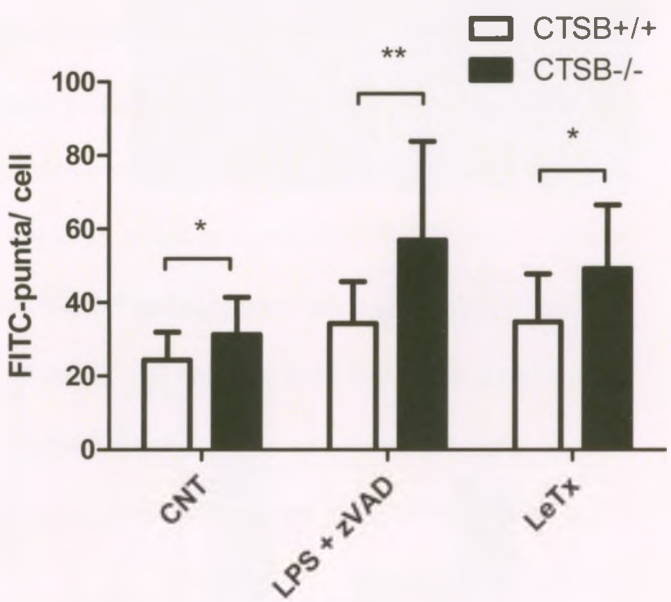

Figure 3.6. CTSB-deficient BMDIM have a defect in autolysosome efflux.

BMDIM from C57BL/6j ($CTSB^{+/+}$) or CTSB-deficient ($CTSB^{-/-}$) mice were incubated with cell culture media containing DQ-BSA ® Green (10 µg/ml) for 15 min at 37 °C in 5% CO2. Cells were washed with PBS and incubated further with fresh cell culture media for 45 min to ensure that DQ-BSA had reached the lysosomal compartment. Cells were then further incubated with media for 6 H and then fixed with 4% formaldehyde. Immunofluorescent staining was performed using anti-LC3 primary antibodies biotinylated anti-rabbit IgG secondary antibodies and TexasRed-avidin D. Cells were visualized using Olympus fluorescent microscope at 600 x magnification (A). Data represents one of two independent experiments. After the same treatment with DQ-BSA ® Green as above, cells were then fixed with 4% formaldehyde at the indicated time points. Cells were visualized using Zeiss LSM510 META confocal microscope at 630x magnification and ZEN software (B). [Scale bar: 11µM]. *Dotted lines* indicate the cell margin. Data represents one of two independent trials. DQ-BSA puncta per cell were counted (C). Minimum of 20 cells were counted at random. Mean±S.E.M. ns: not significant, ***: $P < 0.0001$. Student's t-test.

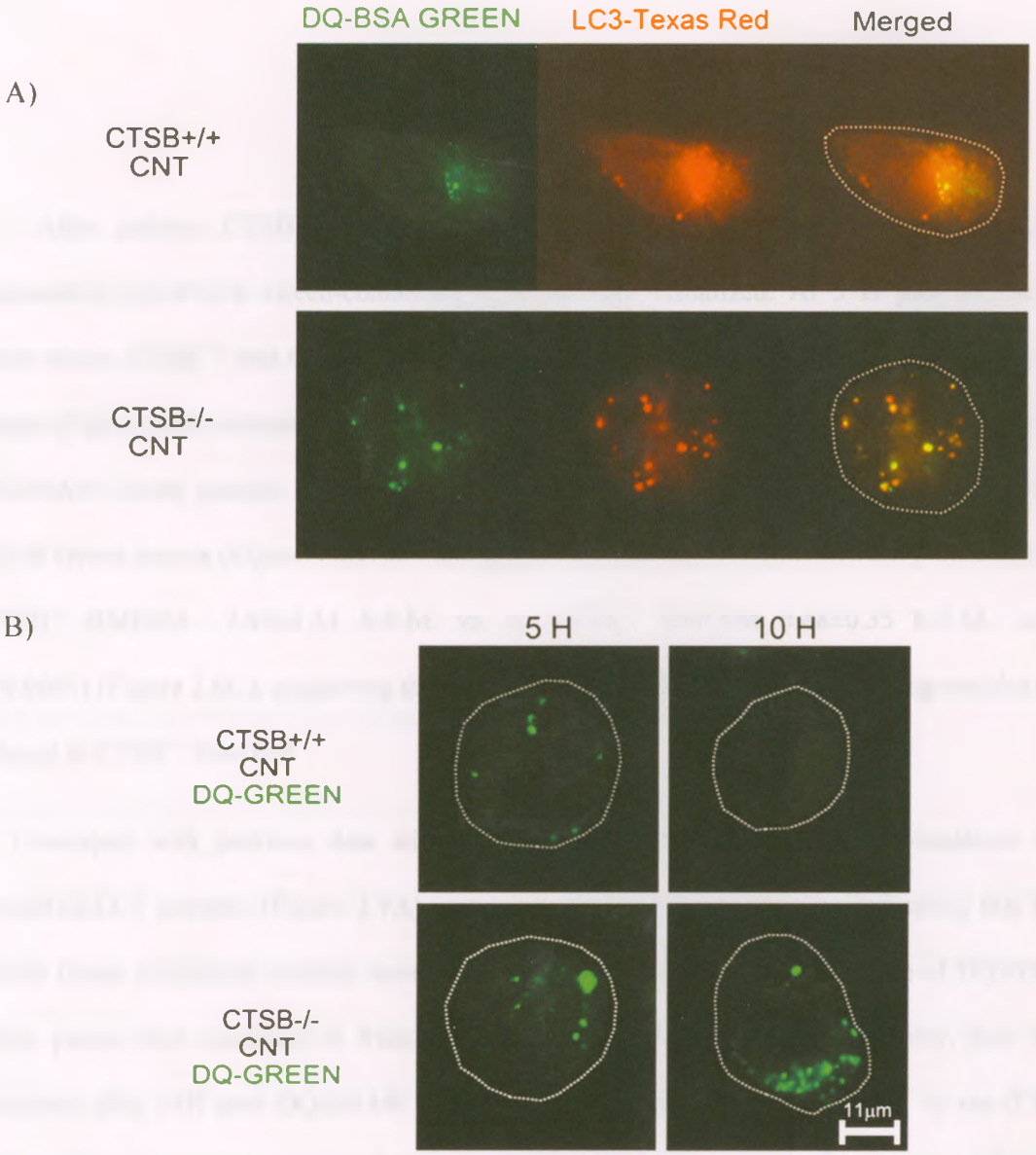
DQ-BSA GREEN
LC3-Texas Red
Merged
A)
CTSB+/+
CNT
CTSB-/-
CNT
B)
5 H
10 H
CTSB+/+
CNT
DQ-GREEN
CTSB-/-
CNT
DQ-GREEN
11µm
C)
ns
***
CTSB +/+
CTSB-/-
DQ-BSA punta/ cell
20
15
10
5
0
5H
10H
Time

After pulsing $CTSB^{+/+}$ and $CTSB^{-/-}$ BMDM with DQ-BSA® Green for 15 min, dequenched DQ-BSA® Green-containing vesicles were visualized. At 5 H post DQ-BSA® Green pulse, $CTSB^{+/+}$ and $CTSB^{-/-}$ BMDIM retained dequenched DQ-BSA ®Green-containing puncta (Figure 3.6B column 1 & 3.6C). At 10 H, $CTSB^{+/+}$ BMDIM almost completely cleared DQ-BSA® Green puncta; however, $CTSB^{-/-}$ BMDIM still harbored larger fluorescent DQ-BSA® Green puncta (Figure 3.6B) and had greater numbers of DQ-BSA®Green puncta at 10 H ($CTSB^{-/-}$ BMDIM 7.95±1.53 S.E.M. vs. to $CTSB^{+/+}$ BMDIM 0.88±0.35 S.E.M., n=40, $P<0.0001$) (Figure 3.6C), suggesting that clearance of DQ-BSA® Green containing vesicles was delayed in $CTSB^{-/-}$ BMDIM.

Consistent with previous data with BMDIM, DQ-BSA®Green puncta co-localized with TexasRed-LC3 markers (Figure 3.7A) in primary peritoneal macrophages indicating that DQ-BSA® Green containing vesicles were autolysosomes. In addition, the clearance of DQ-BSA® Green puncta was examined in freshly isolated peritoneal macrophages. However, they were examined after 24H post DQ-BSA® Green load instead of after 10H in order to see if DQ-BSA® Green vesicles still persisted (Figure 3.7B & 3.7C). Indeed, $CTSB^{-/-}$ cells were delayed in clearing DQ-BSA® Green puncta than $CTSB^{+/+}$ cells at 24 H ($CTSB^{-/-}$ macrophages 8.47±0.93 S.E.M. compared to $CTSB^{+/+}$ macrophages 3.04±0.57 S.E.M., n=30, $P<0.0001$) (Figure 3.7B & 3.7C).

The role of CTSB in autolysosome efflux was also examined in the human monocytic cell line THP-1, using DQ-BSA® Red in the presence or absence of the membrane permeable CTSB inhibitor CA074-Me. THP-1 cells were pulsed with DQ-BSA® Red for 15 min, then dequenched DQ-BSA® Red-containing vesicles were visualized. At 20 H post DQ-BSA® Red pulse, CA-074-Me treatment caused a delay in the clearance of DQ-BSA® Red puncta (Figure 3.8A). DQ-

BSA® Red fluorescence was also quantified by flow cytometry analysis. After 21 H post load, THP-1 cells alone showed lower DQ-BSA® Red fluorescence than CA074-Me treated cells (THP-1 4.37±0.02 S.E.M. compared to THP-1 with CA074-Me 9.93±0.06 S.E.M., n=2, P<0.0001) (Figure 3.8B). Hence, in the presence of CA074-Me, the rate of DQ-BSA® Red clearance was delayed when compared with that of non-treated cells. Overall, these results suggest that CTSB is involved in the efflux of DQ-BSA® containing vesicles such as autoysosomes, in human and mouse macrophages.

3.2. Function of Autolysosome efflux

3.2.1. Autolysosome efflux and autophagy-induced cell death

Although autophagy is a cell survival mechanism during stress or starvation, aberrant activation of autophagy was shown to be involved in cell death, known as autophagic cell death[52-53]. To examine if there is a correlation between autolysosome efflux and cell death, BMDIM were treated with LPS+zVAD or LeTx, or cultured in serum-free media. Treatment with LPS+zVAD was shown to induce autophagic cell death in primary peritoneal macrophages[16]. $CTSB^{+/+}$ or $CTSB^{-/-}$ BMDIM were treated with LPS (1ug/ml)+zVAD (50uM) for 24 H and cell viability was determined using an MTT (3-(4,5-Dimethylthiazol-2-yl)-2,5-diphenyltetrazolium bromide, a tetrazole) assay. MTT, a yellow tetrazole, is reduced to purple crystals in mitochondria of living cells [94]. $CTSB^{-/-}$ BMDIM were susceptible to LPS+zVAD-induced cell death but $CTSB^{+/+}$ BMDIM were not susceptible ($CTSB^{-/-}$ BMDIM 17.76% ±2.55 S.E.M. vs. $CTSB^{+/+}$ BMDIM 92.81% ±5.49 S.E.M., n=7, P<0.0001) (Figure 3.9A).

Figure 3.7. CTSB-deficient peritoneal macrophages have a defect in autolysosome efflux

Peritoneal macrophages isolated from C57BL/6j ($CTSB^{+/+}$) or CTSB-deficient ($CTSB^{-/-}$) mice were incubated with cell culture media containing DQ-BSA ® Green (10 µg/ml) for 15 min at 37 °C in 5% CO2. Cells were washed with PBS and incubated further with fresh cell culture media for 45 min to ensure that DQ-BSA had reached the lysosomal compartment. Cells were then further incubated with media for 6 H and then fixed with 4% formaldehyde. Immunofluorescent staining was performed using anti-LC3 primary antibodies biotinylated anti-rabbit IgG secondary antibodies and TexasRed-avidin D. Cells were visualized using Olympus fluorescent microscope at 600 x magnification (A). Data represents one of two independent experiments. After the same treatment with DQ-BSA ® Green as above, cells were then fixed with 4% formaldehyde at the indicated time points. Cells were visualized using Olympus microscope at 600x magnification (B). [Scale bar: 11µM]. *Dotted lines* indicate the cell margin. Data represents one of two independent trials. DQ-BSA puncta per cell were counted (C). Minimum of 20 cells were counted. Mean±S.E.M. ns: not significant , ***: $P < 0.0001$. Student's t-test.

A)

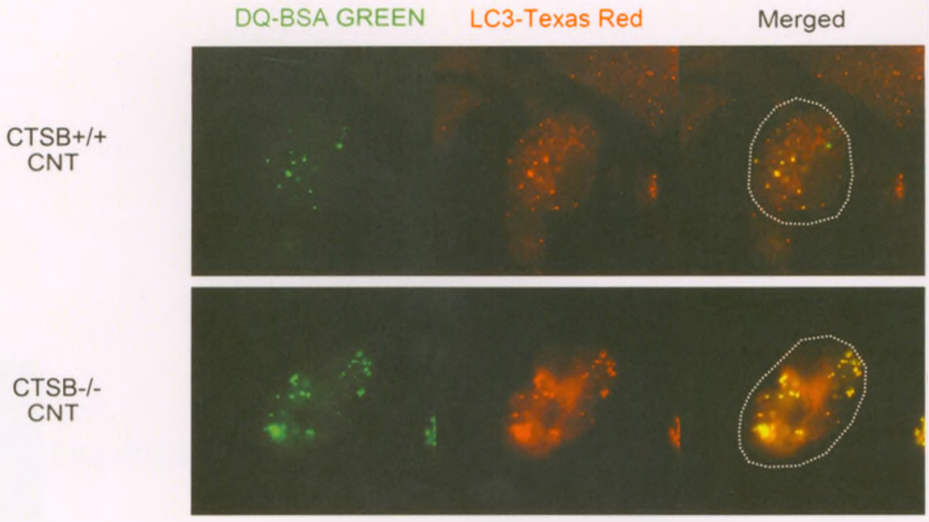
DQ-BSA GREEN
LC3-Texas Red
Merged
CTSB+/+
CNT
CTSB-/-
CNT

B)

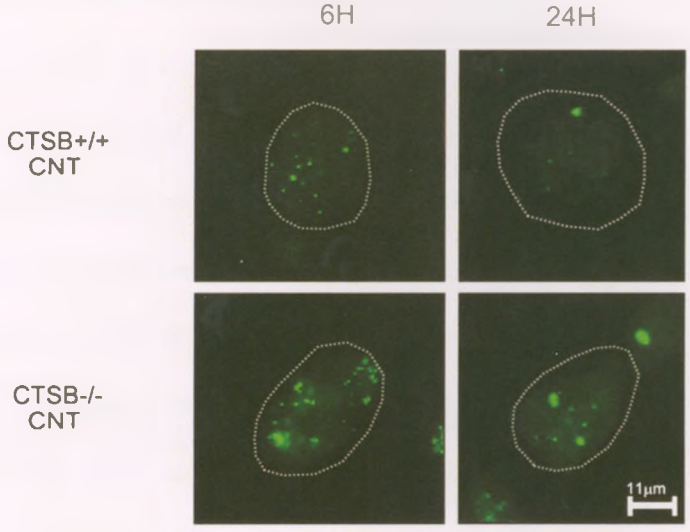
6H
24H
CTSB+/+
CNT
CTSB-/-
CNT
11µm

C)

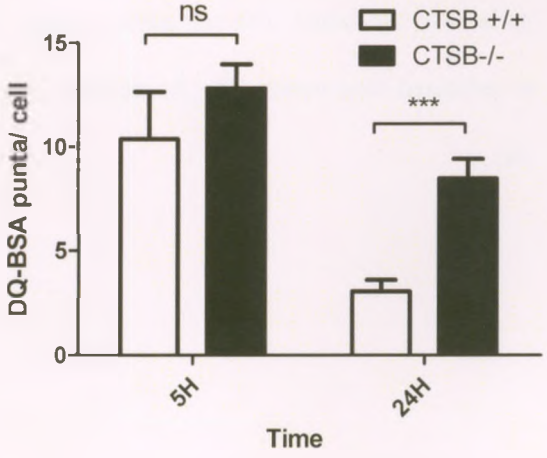
ns
CTSB +/+
CTSB-/-
***
DQ-BSA punta/ cell
15
10
5
0
5H
24H
Time

Figure 3.8. CTSB inhibition shows defect in autolysosome efflux (published in[95]). THP-1 cells were incubated with RPMI media containing DQ-BSA (10 μg/ml) for 15 min at 37 °C in 5% CO_2. Cells were washed and incubated further with cell culture media for 45 min to ensure that DQ-BSA had reached the lysosomal compartment. Cells were then further incubated with fresh cell culture media in the presence or absence of CA074-Me (50 μM). Cells were then plated on coverslips and fixed with 4% formaldehyde at the indicated time point. The fluorescent products of DQ-BSA were imaged using the Bio-Rad Radiance 2000 two-photon confocal microscope at 630X and LaserSharp 2000 software (A). *Dotted lines* indicate the cell margin. For flow cytometry analaysis, THP-1 cells were pretreated with DQ-BSA as above in (A) and cells were incubated with cell culture media with or without CA074-Me (50 μM), then harvested at indicated time points. The fluorescence mean for each population was analyzed using Flow Jo (B).

A)

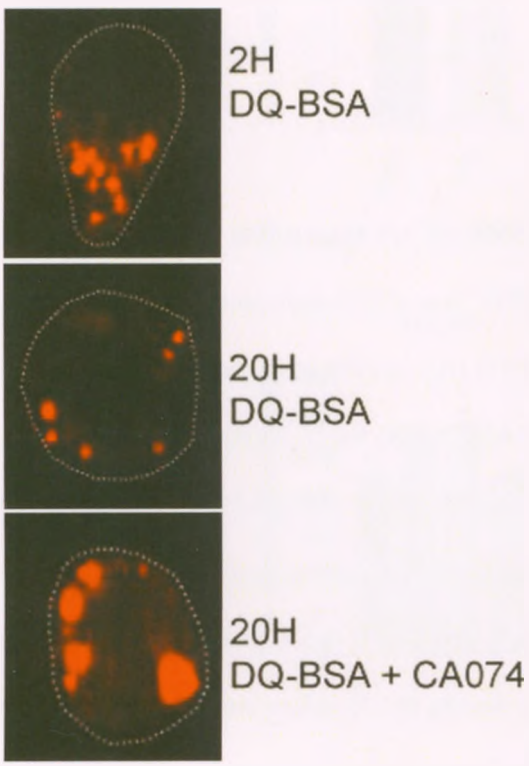
2H
DQ-BSA
20H
DQ-BSA
20H
DQ-BSA + CA074

B)

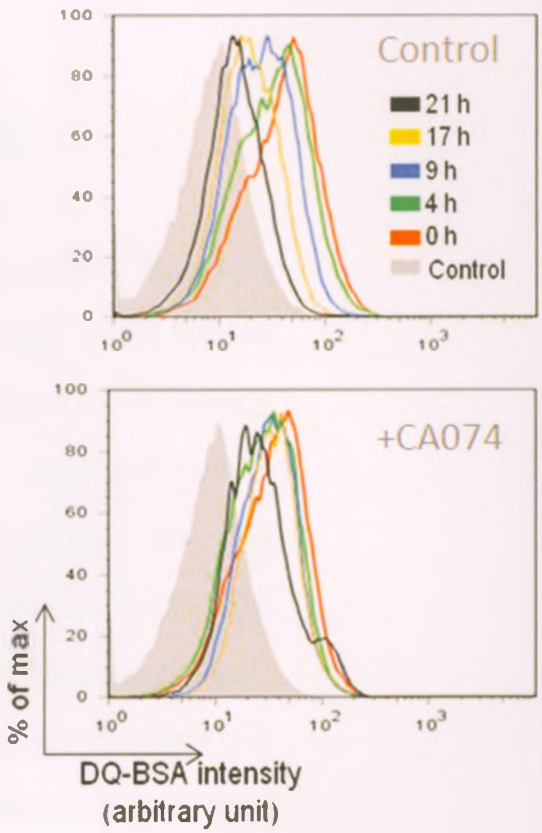
Control
21 h
17 h
9 h
4 h
0 h
Control
+CA074
% of max
DQ-BSA intensity
(arbitrary unit)

Figure 3.9. CTSB-deficient BMDIM are susceptible to LPS+zVAD-induced cell death. BMDIM from C57BL/6j ($CTSB^{+/+}$) or CTSB-deficient ($CTSB^{-/-}$) mice were treated with LPS (1ug/ml)+zVAD (50uM) for 24 H (A), or cells were pretreated with Nec-1 (40uM) for 1 H then treated with LPS (1ug/ml)+zVAD (50uM) for 24 H (B). MTT was added 2 H before the end of experiment to determine cell viability (n=3). BMDIM from C57BL/6j ($CTSB^{+/+}$) and CTSB-deficient ($CTSB^{-/-}$) mice were pretreated with Nec-1 (40uM) for 1 H and then treated with LPS (1ug/ml)+zVAD (50uM) for 2 H. The LC3-I and II proteins were examined using Western blot (C). Western blots against p38 were used as loading controls. Densitometric LC3-II/p38 ratios are shown beside the blot. Data represent one of two independent experiments.

A)

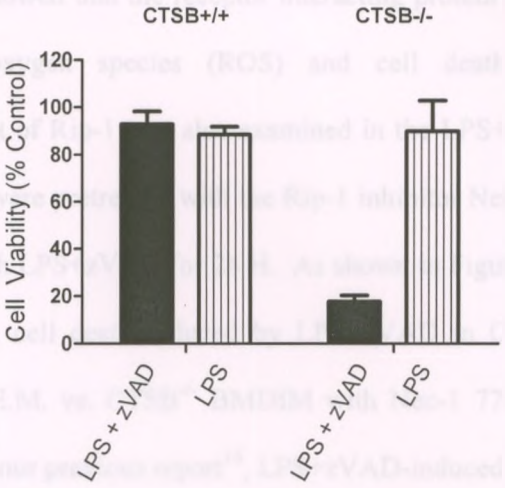
CTSB+/+
CTSB-/-
Cell Viability (% Control)
120
100
80
60
40
20
0
LPS + zVAD
LPS
LPS + zVAD
LPS

B)

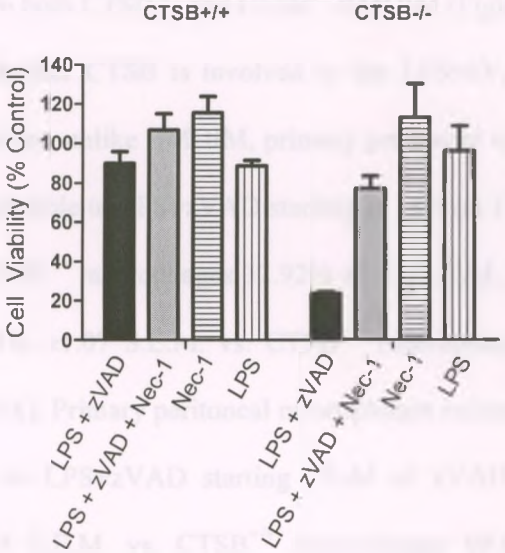
CTSB+/+
CTSB-/-
Cell Viability (% Control)
140
120
100
80
60
40
20
0
LPS + zVAD
LPS + zVAD + Nec-1
Nec-1
LPS
LPS + zVAD
LPS + zVAD + Nec-1
Nec-1
LPS

C)

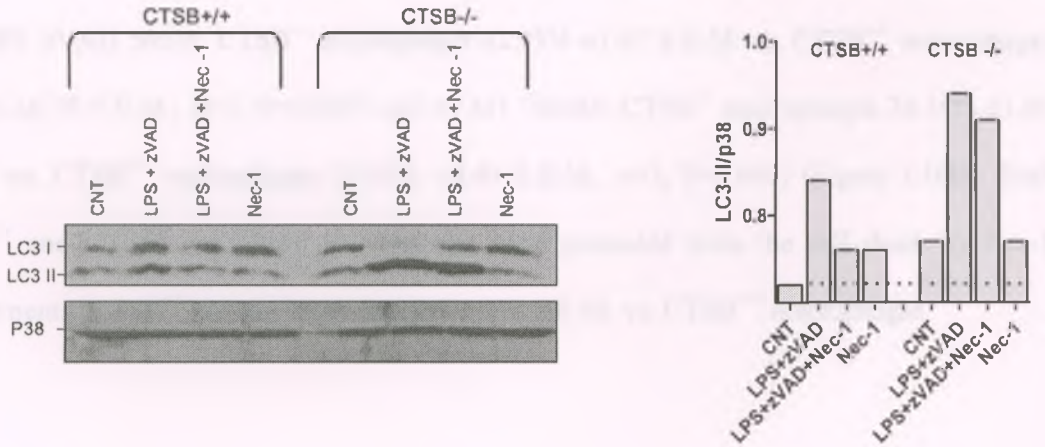
CTSB+/+
CTSB-/-
CNT
LPS + zVAD
LPS + zVAD +Nec -1
Nec-1
CNT
LPS + zVAD
LPS + zVAD +Nec -1
Nec-1
LC3 I
LC3 II
P38
LC3-II/p38
1.0
0.9
0.8
CTSB+/+
CTSB -/-
CNT
LPS+zVAD
LPS+zVAD+Nec-1
Nec-1
CNT
LPS+zVAD
LPS+zVAD+Nec-1
Nec-1

Since our previous study showed that the receptor interacting protein (Rip)-1 is involved in the production of reactive oxygen species (ROS) and cell death in LPS+zVAD-treated macrophages[16], involvement of Rip-1 was also examined in the LPS+zVAD-induced cell death of $CTSB^{-/-}$ BMDIM. Cells were pretreated with the Rip-1 inhibitor Necrostatin 1 (Nec-1; 40uM) for 1 H and then treated with LPS+zVAD for 24 H. As shown in Figure 3.9B, pretreatment with Nec-1 was protective from cell death induced by LPS+zVAD in $CTSB^{-/-}$ BMDIM ($CTSB^{-/-}$ BMDIM 17.76% ±2.55 S.E.M. vs. $CTSB^{-/-}$ BMDIM with Nec-1 77.09% ±6.42 S.E.M., n=3, $P<0.0001$). Consistent with our previous report[16], LPS+zVAD-induced LC3-II accumulation was slightly inhibited by Nec-1 in both $CTSB^{+/+}$ and $CTSB^{-/-}$ BMDIM (Figure 3.9C).

I further examined whether CTSB is involved in the LPS+zVAD-induced cell death in primary macrophages. However, unlike BMDIM, primary peritoneal macrophages isolated from $CTSB^{-/-}$ mice were less susceptible to LPS+zVAD starting at 18H (at 18H: $CTSB^{-/-}$ macrophages 45.17% ±2.02 S.E.M vs. $CTSB^{+/+}$ macrophages 32.92% ±1.54 S.E.M., n=3, P=0.04 and at 24H: $CTSB^{-/-}$ macrophages 42.93% ±1.07 S.E.M. vs. $CTSB^{+/+}$ macrophages 28.74% ±0.79 S.E.M, n=3, P=0.0087) (Figure 3.10A). Primary peritoneal macrophages isolated from $CTSB^{-/-}$ mice also showed less susceptibility to LPS+zVAD starting 25uM of zVAD (zVAD 25uM: $CTSB^{-/-}$ macrophages 86.15% ±1.54 S.E.M. vs. $CTSB^{+/+}$ macrophages 69.04% ±0.45 S.E.M., n=3, P=0.0087. zVAD 50uM: $CTSB^{-/-}$ macrophages 42.93% ±1.07 S.E.M. vs. $CTSB^{+/+}$ macrophages 28.74% ±0.79 S.E.M., n=3, P=0.0087 and zVAD 100uM: $CTSB^{-/-}$ macrophages 34.15% ±1.03 S.E.M. vs. $CTSB^{+/+}$ macrophages 29.01% ±0.49 S.E.M., n=3, P=0.046) (Figure 3.10B). Both $CTSB^{+/+}$ and $CTSB^{-/-}$ peritoneal macrophages were protected from the cell death by Nec-1 pretreatments ($CTSB^{+/+}$ macrophages 34.12% ±1.78 S.E.M. vs. $CTSB^{+/+}$ macrophages

Figure 3.10. LPS+zVAD induced cell death in CTSB$^{+/+}$ and CTSB$^{-/-}$ macrophages.

Peritoneal macrophages isolated from C57BL/6j (CTSB$^{+/+}$) or CTSB-deficient (CTSB$^{-/-}$) mice were pretreated with Nec-1 (40uM) for 1H then treated with LPS (200ng/ml)+zVAD (50 uM) for 24 H (A). The cells were treated with LPS (200ng/mL)+zVAD (50uM) for indicated times (B) or LPS (200ng/mL) and different concentrations of zVAD (C) for 24 H. Cell viability was determined by crystal violet staining. (n=2). Peritoneal macrophages isolated from C57BL/6j wild type (CTSB$^{+/+}$) or CTSB-deficient (CTSB$^{-/-}$) mice were pretreated with Nec-1 (40uM) for 1 H then treated with LPS (200ng/ml)+zVAD (50 uM) for 2 H. LC3-I and LC3-II proteins were analyzed by Western blot (D). Western blots against Actin were used as loading controls. Densitometric LC3-II/Actin ratios are shown beside the blot. Data represent one of two independent experiments. Mean±S.E.M. *$P<0.05$. Student's t-test.

A)

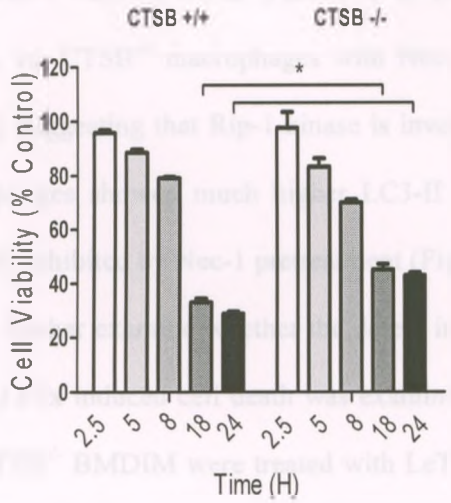
CTSB +/+
CTSB -/-
*
Cell Viability (% Control)
120
100
80
60
40
20
0
2.5
5
8
18
24
2.5
5
8
18
24
Time (H)

B)

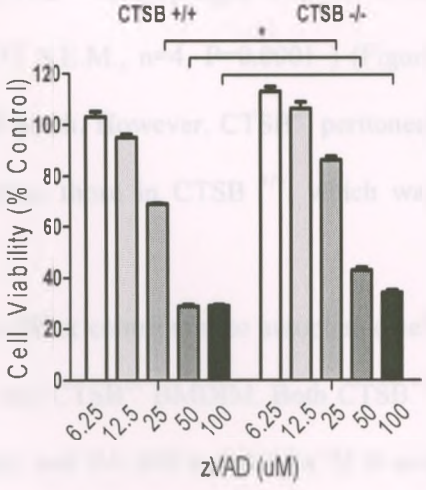
CTSB +/+
CTSB -/-
*
Cell Viability (% Control)
120
100
80
60
40
20
0
6.25
12.5
25
50
100
6.25
12.5
25
50
100
zVAD (uM)

C)

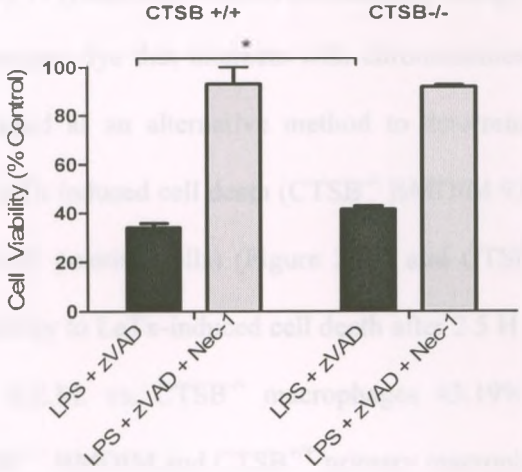
CTSB +/+
CTSB-/-
*
Cell Viability (% Control)
100
80
60
40
20
0
LPS + zVAD
LPS + zVAD + Nec-1
LPS + zVAD
LPS + zVAD + Nec-1

D)

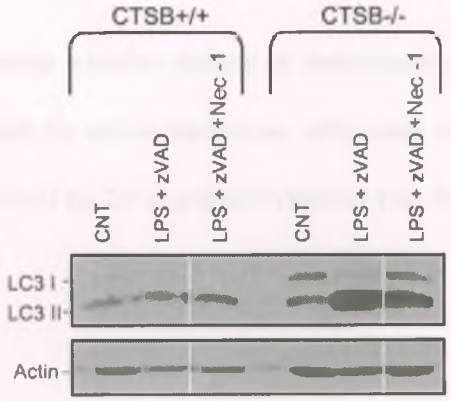
CTSB+/+
CTSB-/-
CNT
LPS + zVAD
LPS + zVAD +Nec -1
CNT
LPS + zVAD
LPS + zVAD +Nec -1
LC3 I
LC3 II
Actin

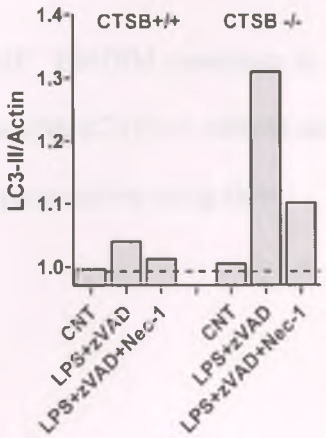
CTSB+/+
CTSB -/-
LC3-II/Actin
1.4
1.3
1.2
1.1
1.0
CNT
LPS+zVAD
LPS+zVAD+Nec-1
CNT
LPS+zVAD
LPS+zVAD+Nec-1

with Nec-1 92.94% ±7.02 S.E.M., n=4, P=0.0002 and CTSB$^{-/-}$ macrophages 41.64% ±1.29 S.E.M. vs. CTSB$^{-/-}$ macrophages with Nec-1 91.60% ±0.77 S.E.M., n=4, P=0.0001) (Figure 3.10C), suggesting that Rip-1 kinase is involved in the cell death. However, CTSB$^{-/-}$ peritoneal macrophages showed much higher LC3-II protein level than those in CTSB $^{+/+}$, which was partially inhibited by Nec-1 pretreatment (Figure 3.10D).

To further examine whether the defect in autolysosome efflux contributes to autophagic cell death, LeTx induced cell death was examined in CTSB$^{+/+}$ and CTSB$^{-/-}$ BMDIM. Both CTSB$^{+/+}$ and CTSB$^{-/-}$ BMDIM were treated with LeTx (LF 250 ng/ml and PA 500 ng/mL) for 24 H and cell viability was determined by PI (propidium iodide) permeability using flow cytometry. PI is a membrane impermeable fluorescent dye that interacts with chromosomes when a cell loses its membrane integrity. PI was used as an alternative method to determine cell death. CTSB$^{-/-}$ BMDIM were susceptible to LeTx induced cell death (CTSB$^{-/-}$ BMDIM 93.25% PI positive cells vs. CTSB$^{+/+}$ BMDIM 26.21% PI positive cells) (Figure 3.11) and CTSB$^{-/-}$ primary peritoneal macrophages showed susceptibility to LeTx-induced cell death after 2.5 H of treatment (CTSB$^{+/+}$ macrophages 90.95% ±2.28 S.E.M. vs. CTSB$^{-/-}$ macrophages 43.19% ±0.81 S.E.M., n=2, P=0.0026) (Figure 3.12). CTSB$^{+/+}$ BMDIM and CTSB$^{+/+}$ primary macrophages were much more resistant to LeTx-induced cell death.

To examine whether defects of autolysosome efflux in CTSB$^{-/-}$ BMDIM contribute to cell death induced by serum starvation, cells were cultured in media with (CNT) or without serum (Serum starved) for 24 H and cell viability was determined by PI permeability using flow

Figure 3.11. CTSB-deficient BMDIM are susceptible to LeTx-induced cell death. BMDIM from C57BL/6j ($CTSB^{+/+}$) or CTSB-deficient ($CTSB^{-/-}$) mice were treated with LeTx (LF 250 ng/ml and PA 500 ng/mL) for 24 H. Cell viability was determined by PI staining followed by flow cytometry (n=1).

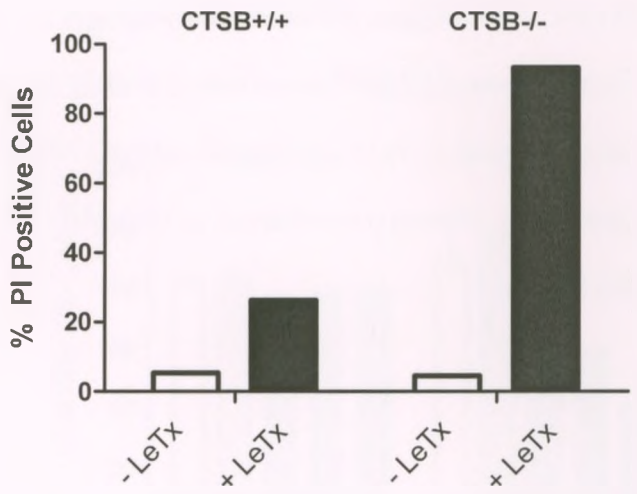
CTSB+/+
CTSB-/-
% PI Positive Cells
100
80
60
40
20
0
- LeTx
+ LeTx
- LeTx
+ LeTx

Figure 3.12. CTSB-deficient peritoneal macrophages are sensitized to LeTx induced cell death. Peritoneal macrophages isolated from C57BL/6j ($CTSB^{+/+}$) or CTSB-deficient ($CTSB^{-/-}$) mice were treated with LeTx (LF 250 ng/ml and PA 1500 ng/mL) for the indicated time points (A) or treated with different concentrations of LeTx (B). Cell viability was determined by crystal violet staining. (n=2)

A)

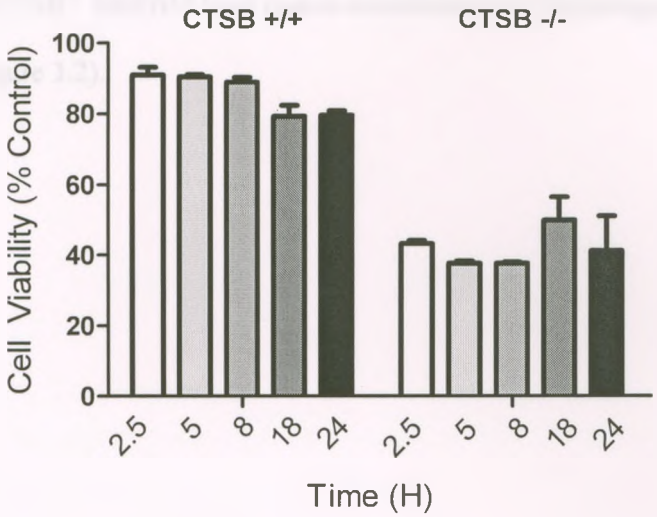
CTSB +/+
CTSB -/-
Cell Viability (% Control)
100
80
60
40
20
0
2.5
5
8
18
24
2.5
5
8
18
24
Time (H)

B)

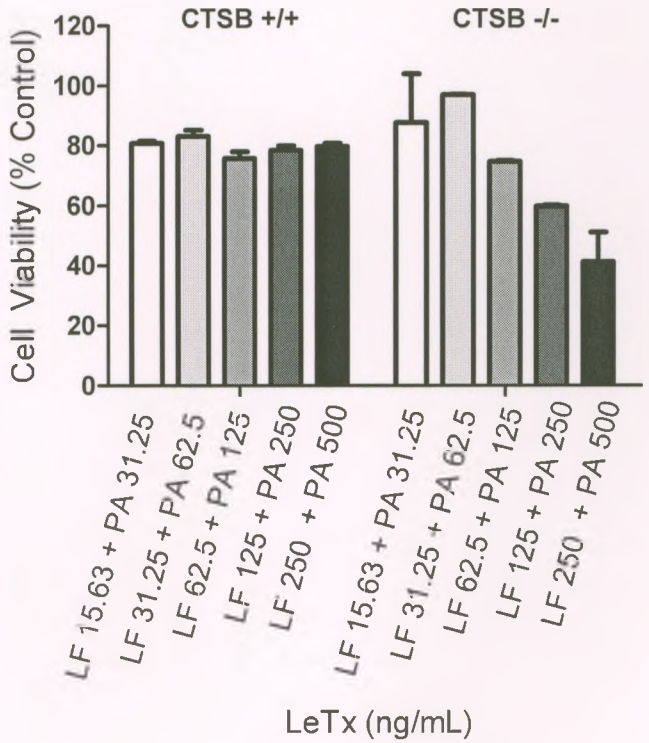
CTSB +/+
CTSB -/-
Cell Viability (% Control)
120
100
80
60
40
20
0
LF 15.63 + PA 31.25
LF 31.25 + PA 62.5
LF 62.5 + PA 125
LF 125 + PA 250
LF 250 + PA 500
LF 15.63 + PA 31.25
LF 31.25 + PA 62.5
LF 62.5 + PA 125
LF 125 + PA 250
LF 250 + PA 500
LeTx (ng/mL)

CTSB $^{+/+}$ and CTSB$^{-/-}$ showed a similar degree of cell death (CTSB$^{+/+}$ macrophages 43.91% ±14.39 S.E.M. vs. CTSB$^{-/-}$ macrophages 32.54% ±2.48 S.E.M., n=2, P=0.512) (Figure 3.13), despite the fact that CTSB$^{-/-}$ BMDIM have higher accumulation of autophagic vesicles during serum starvation (Figure 3.2).

Figure 3.13. CTSB-deficient BMDIM are not sensitized to serum starvation-induced cell death. BMDIM from C57BL/6j ($CTSB^{+/+}$) or CTSB-deficient ($CTSB^{-/-}$) mice were incubated with cell culture media with (CNT) or without serum (Serum Starved) for 24H. Cell viability was determined by PI staining followed by flow cytometry (n=2). Mean±S.E.M. ns: not significant. Student's t-test.

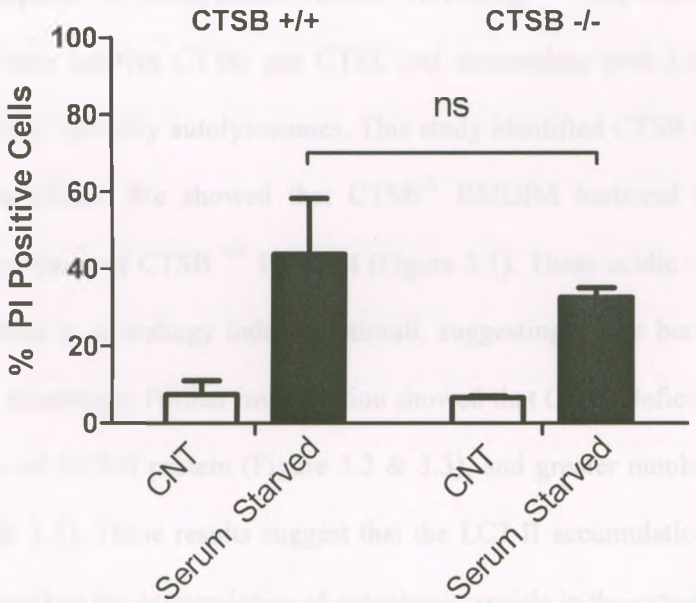
CTSB +/+
CTSB -/-
ns
% PI Positive Cells
100
80
60
40
20
0
CNT
Serum Starved
CNT
Serum Starved

Chapter 4-Discussion

4.1.1 CTSB-mediated autolysosome efflux

In previous studies, CTSB has been suggested to be involved in certain vesicle trafficking[12, 87]. In yeast, inhibition of proteinase B, an orthologue of mammalian CTSB, induces a large accumulation of autophagic vacuoles[86]. CTSB and CTSL (cathepsin L) double knockout mice show large vesicle accumulation in neuronal tissues[87] A recent study also substantiated the role of cathepsins in autolysosme vesicle trafficking[12]. They showed that acinar cells in pancreatitis have inactive CTSB and CTSL and accumulate both LAMP-2 positive and LC3 positive vesicles, possibly autolysosomes. This study identified CTSB as a key player mediating autolysosome efflux. We showed that $CTSB^{-/-}$ BMDIM harbored larger acidic vesicles in comparison to those of $CTSB^{+/+}$ BMDIM (Figure 3.1). These acidic vesicles were increased in size in response to autophagy inducing stimuli, suggesting a link between the observed acidic vesicles and autophagy. Further investigation showed that CTSB deficiency resulted in increased accumulation of LC3-II protein (Figure 3.2 & 3.3), and greater number and size of LC3 punta (Figure 3.4 & 3.5). These results suggest that the LC3-II accumulations that were observed by Western blot reflect the accumulation of autophagic vesicle in the cytosol.

Further investigation revealed that LC3-II staining co-localized with DQ-BSA® containing vesicles (Figure 3.6A & 3.7A). This observation confirmed that 1) In the absence of CTSB, autophagosome and lysosome fusion occurs without any apparent abnormalities and 2) DQ-BSA® containing vesicles are autolysosomes. However, the clearance of DQ-BSA® containing vesicles was delayed in both $CTSB^{-/-}$ BMDIM and primary macrophages when compared with that of wild-type cells (Figure 3.6B, 3.6C, 3.7B and 3.7C), suggesting that CTSB is important in mediating autolysosome efflux.

We also showed that inhibition of CTSB by CA-074Me caused an increase in LC3-II levels and accumulation of autophagic vacuoles[95]. CA-074ME-treated THP-1 cells also showed defects in the clearance of DQ-BSA® Red containing vesicles (Figure 3.8). Since CA-074ME inhibits protease activity and not expression of CTSB, the proteolytic activity of CTSB seems to be important for mediating a proper autolysosome efflux.

However, the absence of CTSB did not completely block autolysosome efflux (Figure 3.6 C & 3.7C), suggesting that there are compensatory mechanisms or/and that CTSB is involved in one of many autolysosome vesicle traffickings. To date, little is known about the mechanisms of autolysosome efflux, except that certain components such as cell membrane cholesterol and SNAREs have been shown to be involved. A potential role of cholesterol in autophagic vesicle trafficking is demonstrated in Niemann-Pick type C (NPC), an autosomal recessive neurodegenerative disease caused by mutations in the *NPC1* or *NPC2* gene(s) involved in intracellular cholesterol transport[96]. Neurons in this disease show accumulation of intracellular cholesterol within LC3-positive vesicles[97] or LAMP-2 positive vesicles[98]. In the brain tissues of NPC afflicted individuals, there are high LC3-II levels, as well as the presence of autophagic vacuole-like structures and MVBs[97]. *NPC1* deficient cells or cells treated with the drug U18666A, a cholesterol synthesis inhibitor which causes a phenotype similar to *NPC1* mutations[99], show defective back-fusion between intraluminal vesicles to the surrounding MVB membrane[100]. Since the MVB intraluminal membrane back fusion process in NPC1 deficient cells or U1866A-treated cells is defective, a proper cholesterol homeostasis could be important for autolysosome efflux. Congruent with the observations in *NPC1* deficient cells, alveolar epithelial type II cells treated with the membrane cholesterol-depleting agent methyl-β-cyclodextrin[101] have less ability to fuse with lamellar bodies[102] and accumulation of autophagic

vesicles within the cytosol[103]. These studies collectively suggest that cholesterol is a possible component regulating autolysosome efflux.

The involvement of membrane cholesterol in vesicle trafficking has been associated with SNAREs. Secretory vesicles are preferentially docked to sites on membrane sheets that contain clusters of syntaxin 1 and SNAP-25, and the integrity of these clusters are maintained by cholesterol[40]. Chintagari *et al.* showed that upon cholesterol depletion by methyl-β-cyclodextrin, the cluster of SNAREs such as SNAP-23 or syntaxin 2 was disrupted and formation of the fusion pore was inhibited. Thus, these data suggest that the maintenance of proper SNARE protein clusters by cholesterol is essential for intracellular vesicle trafficking. Therefore, *NPC1* deficient cells may be unable to maintain the SNARE protein clusters properly, resulting in defective autophagy vesicle trafficking.

In our previous study, CTSB was shown to be involved in TNF-containing cargo vesicle trafficking to the plasma membrane, which is a SNARE-mediated process[88] (Figure 4.1). Q-SNAREs, such as syntaxin 6, syntaxin 7 and Vti1b of pro-TNF-containing vesicles and R-SNARE VAMP3 on recycling endosomes are important for their fusion[104]. Subsequently, TNF-containing vesicles fuse to the plasma membrane and the process requires VAMP 3 on TNF-containing vesicles and the Q-SNARE complex of the plasma membrane, comprised of syntaxin 4 and SNAP-23[105]. Post-translational modifications of SNARE proteins and the binding of regulatory proteins are important for SNARE fusion complex formation[106-107]. Since CTSB has been shown to be involved in both transcription and post-translational protein processes for proteins such as prorenin[108], thyroglobulin[109] and other proteinases[110], CTSB was proposed to possibly regulate SNARE components either at the transcriptional or post-translational levels to mediate TNF-containing vesicle trafficking to plasma membrane.

Figure 4.1. A diagram illustrating involvement of CTSB in vesicle trafficking. CTSB is involvement TNF-α vesicle trafficking to plasma membrane and back fusion of intraluminal vesicles to release LeTx into the cytosol. In this study, CTSB has been shown to be involved in autolysosome efflux. In the absence of CTSB, these processes are blocked.

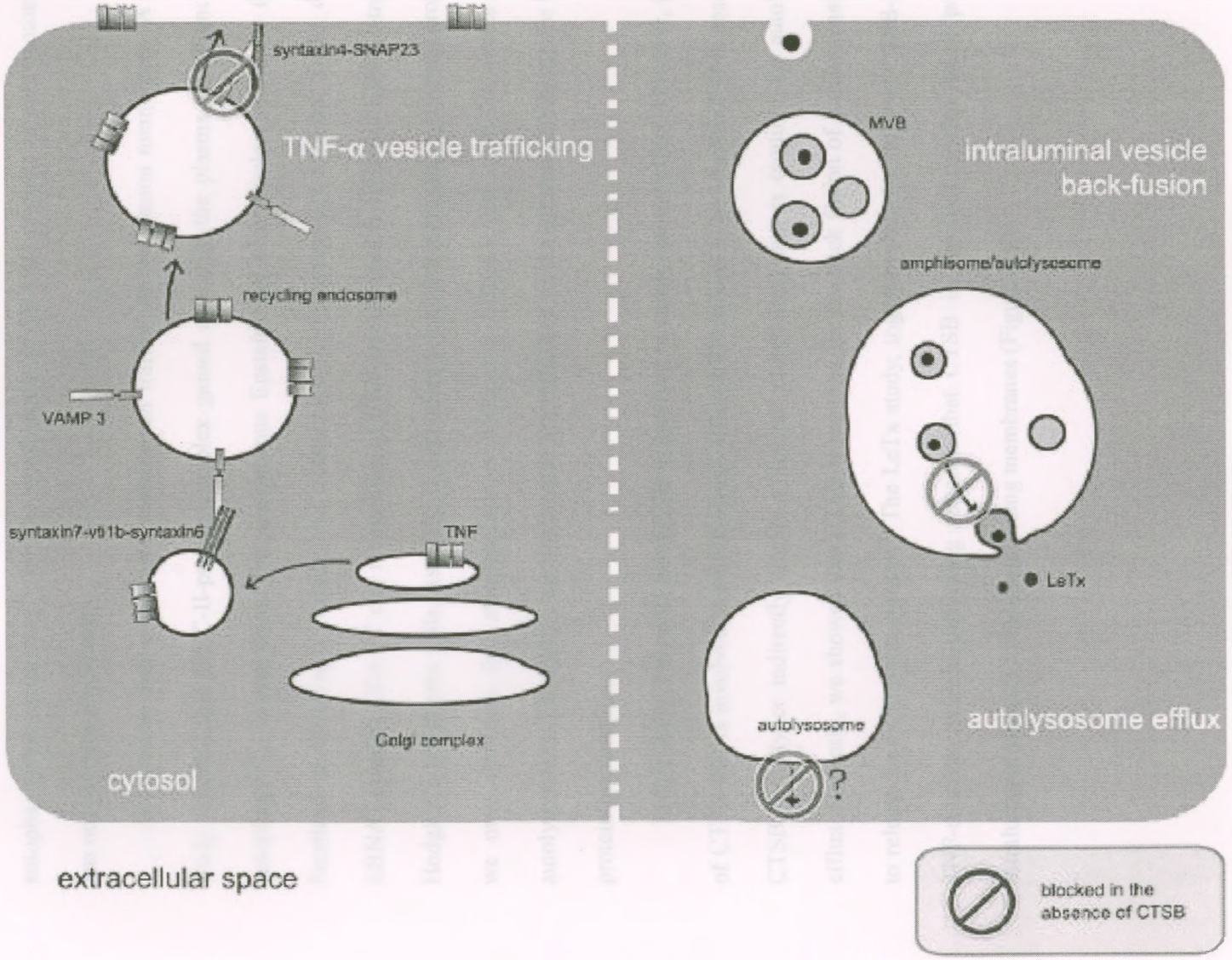
syntaxin4-SNAP23
TNF-α vesicle trafficking
recycling endosome
VAMP 3
syntaxin7-vti1b-syntaxin6
TNF
Golgi complex
cytosol
MVB
intraluminal vesicle back-fusion
amphisome/autolysosome
LeTx
autolysosome
autolysosome efflux
?
extracellular space
blocked in the absence of CTSB

Similarly, CTSB may be involved in autolysosome efflux by modulating SNARE components or cholesterol metabolism. SNARE proteins have been demonstrated to be important for autophagosome maturation[41], but the involvement of SNARE proteins in autolysosome efflux has not yet been elucidated.

It is known that autophagic vesicles can traffick to the plasma membranes. A previous study reported that MHC-II-protein complex gained access to the plasma membrane through autophagy[111]. It was found that endogenous Epstein-Barr virus nuclear antigen 1 (EBNA1) localized to autophagic vesicles and treatment with the autophagy inhibitor 3-MA decreased EBNA1-specific CD4+ T cell recognition of EBV-transformed B cells and EBNA1-transfected Hodgkin's lymphoma cells. As MHC-II-dependent presentation requires lysosomal proteases[112], we may speculate that autophagosomes containing EBNA1 fuse with lysosomes to form autolysosomes. Ultimately, autolysosomes are trafficked to the plasma membrane for MHC-II-protein presentation.

In this study, I showed that CTSB is involved in autolysosome efflux. However, the target of CTSB that is involved in autolysosome efflux still remains to be identified. It is possible that CTSB directly or indirectly targets a luminal molecule(s) that is required for autolysosome efflux. Recently, we showed that CTSB is required for the back fusion of intralumenal vesicles to release LeTx into the cytosol[95]. The LeTx study, together with the study of CTSB-mediated TNF-α cargo vesicle trafficking suggests that CTSB is involved in the fusion process of intralumenal vesicles to the surrounding membranes (Figure 4.1).

4.1.2. Limitations

CTSB$^{-/-}$ BMDIM and primary macrophages showed larger vesicles (Figure 3.1, 3.4A, 3.5A, 3.7B, 3.8B & 3.9A). Similarly, *NPC1* deficient neurons also show accumulation of large LAMP-1 positive intracellular vesicles[113] and Chinese hamster ovary (CHO) cells treated with U18666A show larger and brighter fluorescing LC3-II puncta than non-treated cells[114]. These studies suggest that the large vesicles are a feature of cells with defective autolysosome efflux.

Unfortunately, this study did not fully address whether autophagosome/autolysosome formation (influx) was enhanced in the absence of CTSB due to limited time. One of the methods to measure autophagy influx is examining LC3-II turnover in the presence and absence of lysosomal degradation by Western blots[25]. Preventing lysosomal degradation can be achieved by treatment with agents that block fusion of autophagosomes with lysosomes such as vinblastin, a chemical inhibitor that blocks lysosomal fusion by preventing microtubule-dependent transport of lysosomes[115].

This study also did not address whether LC3-II degradation in autolysosomes were targeted by CTSB. In order to investigate this question, electron microscopy (EM) gold labeling using antibodies against LC3 could be done to see whether autophagosomes/autolysosomes have greater abundance of LC3 within the lumen or on the surfaces. If there are greater amounts of LC3 labeling, we can assess whether CTSB targets LC3-II proteins directly for degradation. HIS tagged-LC3 proteins can be expressed in E.coli and purified using nickel columns. The purified LC3 protein can be incubated with CTSB *in vitro* and run on a SDS-PAGE gel to detect whether proteins are fragmented or not.

4.2. Physiological role of autolysosome efflux

This thesis investigated a possible linkage between autolysosme efflux and cell death. Previous studies have shown that autolysosome efflux is required for the survival of cells and defects in efflux is involved in the pathogenesis of several diseases including Niemann-Pick type C disease (NPC)[116]. To investigate possible physiological roles of autolysosme efflux, I examined whether autolysosome efflux protects macrophages from autophagic cell death.

4.2.1. LPS + zVAD induced cell death

In BMDIM, LPS+zVAD induced Nec-1-dependent autophagic cell death in $CTSB^{-/-}$ cells but not in $CTSB^{+/+}$ cells (Figure 3.9A & 3.9B), which was correlated with LC3-II accumulation (Figure 3.9C). However, $CTSB^{-/-}$ primary peritoneal macrophages were slightly less sensitive to LPS+zVAD induced cell death than $CTSB^{+/+}$ primary peritoneal macrophages (Figure 3.10A, B & 3.10 C), which was not correlated with the LC3-II accumulations observed in these cells (Figure 3.10D). These results indicate that defective autolysosome efflux *per se* in primary peritoneal macrophages was not the main contributor of the cell death. The reason for the different responses in between BMDIM and primary peritoneal macrophages is not clear. However, it is possible that primary peritoneal macrophages were also susceptible to non-autophagic cell death induced by LPS+zVAD and masked the effects of autophagic cell death. In fact, multiple pathways have been shown to be involved in LPS+zVAD-induced macrophage death[92, 117]. Also, unlike primary macrophages, BMDIM were obtained through stably transfecting the oncogenes c-Myc and c-Raf. Could these oncogenes render BMDIM resistant to non-autophagic cell death such as apoptosis and autophagic cell death which was eminent in

BMDIM? These questions could be addressed by specifically preventing autophagic or non-autophagic cell death. I have tested the chemical autophagy inhibitor 3-MA with inconclusive results. 3-MA failed to prevent LC3-II accumulation (Appendix A1) and cell death induced by the autophagy stimuli tested (data not shown). In fact, a recent study showed that 3-MA can be a promoter of autophagy after 9 hours of treatment[118]. In this study, cell death was measured after 24 hours of treatment, thus, autophagy could have been rather induced by 3-MA. Using siRNA against ATGs could have been an alternative approach to prevent autophagic cell death. We are currently optimizing siRNA protocol to inhibit expression of ATGs and no data is available at this moment.

The difference in cell death between primary and immortalized macrophages may also be due to ROS regulation. Yu *et al.* showed that zVAD-induced autophagy in L929 fibroblasts can selectively degrade catalase, an ROS scavenger, which results in greater accumulation of ROS followed by necrotic cell death[17]. In primary macrophages, LPS+zVAD was shown to induce Rip-1-dependent ROS production[16]. Many tumor cells express higher antioxidants to avoid oxidative damage[119-121]. Thus, $CTSB^{+/+}$ BMDIM may be protected from ROS-mediated necrotic cell death whereas primary macrophages are susceptible. Indeed, acute myeloid leukemia cells are resistant to TNFα due to enhanced antioxidant responses, while primary monocytes were susceptible to TNFα-induced cell death[122].

It was unexpected to find that $CTSB^{+/+}$ primary macrophages were slightly more susceptible to LPS+zVAD induced cell death than $CTSB^{-/-}$ cells. Cathepsin B has been reported to mediate certain caspase-independent cell death pathways[123]. Non-small cell lung cancer cells treated with microtubule stabilizing agents induces caspase-independent cell death and inhibition of cathepsin B results in protection against the drug induced cell death. As mentioned before,

LPS+zVAD induced cell death in macrophages involves multiple pathways[92, 117]. Hence, LPS+zVAD may have partially induced CTSB-dependent cell death pathway and the absence of CTSB may have provided some protection against the cell death.

4.2.2. LeTx induced cell death

Next I examined whether defects of autophagy efflux contribute to LeTx-induced cell death. Indeed, $CTSB^{-/-}$ BMDIM and primary peritoneal macrophages accumulated more autolysosomes after LeTx treatment (Figure 3.2A & 3.3.A) and were more susceptible to LeTx-induced cell death than $CTSB^{+/+}$ cells (Figure 11 & 12). These observations support our hypothesis that proper regulation of autolysosome efflux prevents autophagic cell death. However, it still needs to be confirmed whether the observed cell death is *bona fide* autophagic cell death. Experiments examining whether LeTx-induced cell death was prevented in $CTSB^{-/-}$ cells by knocking down beclin-1 or ATG-5 using siRNA[19] could provide a conclusive evidence for the hypothesis. LeTx induces rapid caspase-1 activation and cell death through activating the NALP1b receptor in certain in-bred mouse strains including 129/Svj and Balb/c, but not in C57BL/6, due to differences in NALP1b alleles[124]. Since $CTSB^{-/-}$ mice were generated using embryonic stem cells with 129/Svj genetic background, it may be possible that $CTSB^{-/-}$ mice still harbor the NALP1b allele from 129/Svj. Since NALP1b-induced cell death can be inhibited by the proteasome inhibitor MG132[125], we examined whether LeTx-induced cell death in $CTSB^{-/-}$ macrophages could be prevented by MG132. In fact, MG132 was able to prevent LeTx-induced cell death in $CTSB^{-/-}$ BMDIM (Appendix A2), suggesting that cell death could be mediated through NALP1b. More definitive studies such as genotyping the NALB1b allele or examining the effects of caspase-1 inhibitors or autophagy inhibitors are required to make a conclusion.

4.2.3. Serum Starvation-induced cell death

It is generally accepted that autophagy is a cell survival mechanism during serum starvation[14, 44]. However, in certain circumstances, autophagy enhances cell death. For example, inhibition of autophagy with PI3K inhibitor LY294002 protected PC12 cells from serum starvation-induced cell death [126]. In addition, serum starvation mainly induces apoptosis [127], and CTSB is an important player in apoptosis[67, 128]. In this study, serum starvation caused about 40% cell death in both $CTSB^{+/+}$ and $^{-/-}$ macrophages (Figure 3.14), although LC3-II was more highly accumulated in $CTSB^{-/-}$ serum starved cells (Figure 3.2B). It is difficult to determine whether the serum starvation-induced cell death observed in macrophages is due to autophagy or apoptosis. This complexity is due to the dual roles of autophagy in both cell death and survival. Therefore, CTSB deficiency may negatively and positively contribute to apoptosis and autophagic cell death, respectively. Further detailed experiments such as examining cell death after specifically inhibiting apoptosis or autophagy may provide conclusive evidence regarding the role of autolysosome efflux in autophagic cell death in $CTSB^{-/-}$ macrophages. Apoptosis can be inhibited by BAX siRNA or zVAD treatments.

4.2.4. CTSB-mediated autolysome efflux is required for anthrax toxin receptor 2-mediated anthrax toxin delivery into the cytoplasm.

Our lab showed that autolysosome efflux plays an important role in LeTx delivery to the cytosol. LeTx is one of the key virulence factors secreted by *Bacillus anthracis*, the causative agent of anthrax[129-130]. LeTx is composed of LF and PA. LF is a metalloproteinase and in certain mouse cells, induces necrosis by activating NACHT-leucine-rich repeat and pyrin domain-

containing protein 1b (NALP1b)[124]. LF also directly cleaves the mitogen-activated protein kinase kinases (MEKs) and causes inactivation of these proteins. PA functions as a cytoplasmic transporter that delivers LF to the cytosol, and is responsible for inducing autophagy[95] which is required for LF delivery to cytosol. Incorporation of LF into the cytoplasm is initiated by the binding of PA to the host surface through interacting with either of two known receptors: anthrax receptor(ANTXR)1[131] and ANTXR2[132]. Although ANTXR1 and -2 share high amino acid sequence homology (~60% in extracellular domains and ~68% in the first 145 residues of cytoplasmic domain) and post-translational modifications such as palmitoylation and ubiquitination[133-134], the pH thresholds for PA to form a transmembrane pore are different in these two receptors [135-136]. It was shown that PA dissociates from ANTXR2 and forms a pore at a lower pH than that required for ANTXR1. Our recent study showed that LeTx is delivered to autolysosomes, and CA-074Me treatment blocked autolysosome efflux and LF translocation to cytosol in ANTXR1 knockdown cells but not in ANTXR2 knockdown[95]. This suggested that cathepsin B-mediated autolysosome efflux is involved in the delivery of ANTXR2-associated LF into the cytoplasm. Further investigations are required to identify roles of autolysosome efflux as no other roles of autolysosome efflux have been identified to this date.

4.3. Future directions

In addition to the experiments suggested above, the following experiments will unravel the role of CTSB in autolysosome efflux and its physiological roles.

4.3.1. CTSB protease activity and autolysosome efflux

CTSB has two peptidase activities depending on pH: exopeptidase activity in low pH and endopeptidase activity in neutral or higher pH[137]. By elucidating which protease activity of CTSB is important in autolysosome efflux, we may narrow down whether CTSB is localized to a low pH or neutral pH environment to mediate autolysosome efflux. By using a method previously described, we can generate a CTSB mutant without exopeptidase activity by removing the occluding loop[138]. We could use this mutant to determine whether exopeptidase activity of CTSB is important for autolysosome efflux or not.

4.3.2. Proteases involved in autolysosome efflux

In order to determine whether there are compensatory mechanisms for CTSB in autolysosome efflux, we could investigate whether other proteases are involved as CTSB is a protease itself. One of the potential proteases to investigate is CTSL which is one of the major lysosomal proteases involved in protein catabolism[139]. As mentioned previously, CTSB and CTSL double knockout mice show large vesicle accumulation in neuronal tissues[87]. CTSB and CTSL have been demonstrated to compensate for each other during maturation of the postnatal central nervous system *in vivo*[87]. During reovirus disassembly to generate infectious subvirion particles, removal of both CTSB and CTSL activity by chemical inhibitors or by genetic knockdown completely abrogates disassembly and growth of reovirus while removal of CTSL activity alone only decreases the capacity of cells to support reovirus disassembly. Hence, CTSL may have a compensatory mechanism in the absence of CTSB during autolysosome efflux.

4.3.3. Proteins involved in autolysosome efflux

In the current literature, very limited information is available regarding the mechanism of autolysosome efflux. In order to understand the autolysosome efflux process, we need to identify proteins involved in the process. Proteins known to be involved in vesicular trafficking such as SNAREs and Annexin II will be good candidates to investigate. SNARE proteins are transmembrane proteins that have been extensively documented to be involved in vesicular membrane fusion and exocytosis[140-141]. Autophagic vesicle trafficking also requires SNARE proteins for the autophagosome fusion process[41]. Potential SNARE proteins for autolysosome efflux would be VAMP-7 and syntaxin-4, which are required for lysosome fusion with the plasma membrane[36].

Another potential protein family to investigate for a role in autolysosome efflux are the Annexins. Annexin II is a Ca^{2+} dependent lipid-binding protein that is found on endosomes, plasma membranes and a subset of exocytotic transport vesicles[142]. It is involved in aggregating vesicles by binding to different membranes[142] and has been documented to play a role in the exocytic pathway, as its inhibition disturbs surface transport of apical proteins[143] and insulin-stimulated plasma membrane translocation of GLUT-4[144]. Also, Ca^{2+} levels required for Annexin II to bind to membranes is similar to those needed to promote exocytosis[145]. This suggests that it may facilitate intracellular vesicle binding to the plasma membrane. Annexin II was also reported to associate and co-localize with CTSB in the caveolae, a lipid raft, of tumor cells[79]. This suggests that annexin II and CTSB may also associate with each other intracellularly and possibly be involved in modulating exocytosis. By identifying the proteins involved in autolysosome efflux, we will be able to have a better understanding of autolysosomal vesicle trafficking.

4.4. Conclusion

To date, extensive studies have unraveled the mechanism of autophagy biogenesis and more than thirty ATG genes have been identified. Although it is obvious that the sequestered components of autolysosomes are released into the cytosol to maintain cellular homeostasis, little is known about how autolysosomes are cleared. We named this process "autolysosome efflux" and showed that CTSB is one of the important players in this process. Unfortunately we were unable to find a clear physiological role of autolysosome efflux in autophagic cell death; a definitive conclusion awaits with more detailed studies. Interestingly, we showed that some pathogenic microbes utilize the autolysosome efflux system to deliver toxins into the cytoplasm [95]. Further investigations are required to unravel a detailed mechanism of autolysosome efflux and to determine CTSB targets in the regulation of autolysosome efflux. These future researches will provide better insights into the autophagy life cycle and a better understanding of autophagy process can potentially provide novel therapeutic strategies for treating many diseases caused by defective or overactive autophagy such as neurodegenerative diseases, pancreatitis or cancer.

Appendix

Appendix A1. 3-MA treatment induces LC3-II. BMDIM from CTSB-deficient ($CTSB^{-/-}$) mice were treated with 3-MA (5mM) for 8H. LC3-I and II proteins were analyzed using Western blotting. Western blot against actin was used as loading controls. Data represent one of three independent experiments.

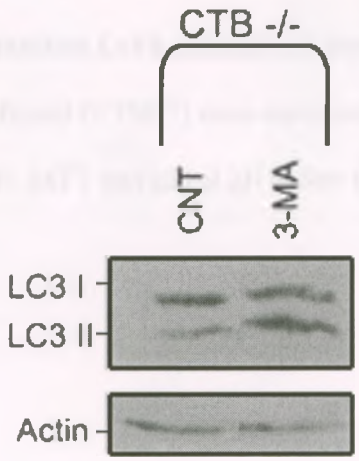
CTB -/-
CNT
3-MA
LC3 I
LC3 II
Actin

Appendix A2. MG132 inhibits LeTx induced cell death in CTSB-deficient BMDIM.

BMDIM from CTSB-deficient ($CTSB^{-/-}$) mice were pretreated with MG132 (10uM) for 1H and treated with LeTx for 2 H. MTT was added 2H before the end of experiment to determine cell viability. (n=3)

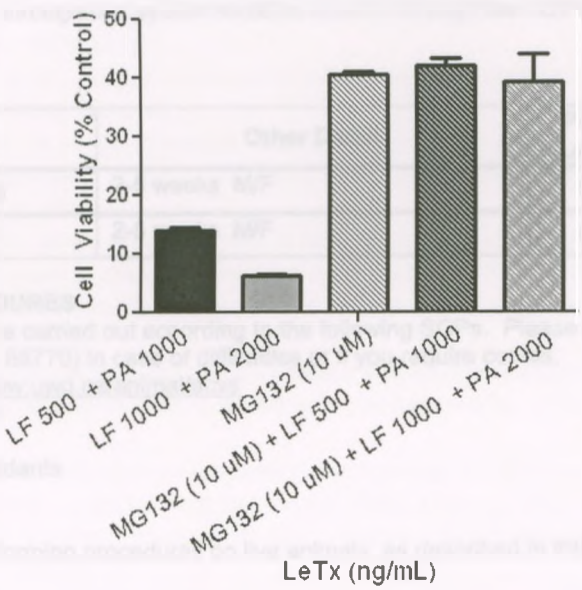
Cell Viability (% Control)
50
40
30
20
10
0
LF 500 + PA 1000
LF 1000 + PA 2000
MG132 (10 uM)
MG132 (10 uM) + LF 500 + PA 1000
MG132 (10 uM) + LF 1000 + PA 2000
LeTx (ng/mL)

Western

March 3, 2008

This is the Original Approval for this protocol
A Full Protocol submission will be required in 2012

Dear Dr. Kim:

Your Animal Use Protocol form entitled:
Anthrax Toxin-Induced Macrophage Cell Cycle Arrest and Death
Funding Agency CIHR - Grant #r3661A05

has been approved by the University Council on Animal Care. This approval is valid from **March 3, 2008 to March 31, 2009.** The protocol number for this project is **#2008-023-03 and replaces #2003-112-12**.

1. This number must be indicated when ordering animals for this project.
2. Animals for other projects may not be ordered under this number.
3. If no number appears please contact this office when grant approval is received.
   If the application for funding is not successful and you wish to proceed with the project, request that an internal scientific peer review be performed by the Animal Use Subcommittee office.
4. Purchases of animals other than through this system must be cleared through the ACVS office. Health certificates will be required.

ANIMALS APPROVED FOR 1 YR.

Species	Strain	Other Detail	Pain Level	Animal # Total for 1 Year
Mouse	C57BL/6	2-5 weeks M/F	C	100
Mouse	Balb/C	2-5 weeks M/F	C	40

STANDARD OPERATING PROCEDURES
Procedures in this protocol should be carried out according to the following SOPs. Please contact the Animal Use Subcommittee office (661-2111 ext. 86770) in case of difficulties or if you require copies.
SOP's are also available at http://www.uwo.ca/animal/acvs
310 Holding Period Post-Admission
320 Euthanasia
321 Criteria for Early Euthanasia/Rodents

REQUIREMENTS/COMMENTS
Please ensure that individual(s) performing procedures on live animals, as described in this protocol, are familiar with the contents of this document.

c.c. Approved Protocol - S-O Kim
Approval Letter - W. '

12/03/08

References

1. Maiuri, M.C., et al., *Self-eating and self-killing: crosstalk between autophagy and apoptosis.* Nat Rev Mol Cell Biol, 2007. **8**(9): p. 741-52.
2. Dice, J.F., et al., *A selective pathway for degradation of cytosolic proteins by lysosomes.* Semin Cell Biol, 1990. **1**(6): p. 449-55.
3. Klionsky, D.J., *Autophagy.* Molecular biology intelligence unit. 2004, Georgetown, Tex. Austin, Tex.: Landes Bioscience ;Eurekah.com. 309 p.
4. Reggiori, F. and D.J. Klionsky, *Autophagy in the eukaryotic cell.* Eukaryot Cell, 2002. **1**(1): p. 11-21.
5. Klionsky, D.J., *Autophagy: from phenomenology to molecular understanding in less than a decade.* Nat Rev Mol Cell Biol, 2007. **8**(11): p. 931-7.
6. Papandreou, I., et al., *Hypoxia signals autophagy in tumor cells via AMPK activity, independent of HIF-1, BNIP3, and BNIP3L.* Cell Death Differ, 2008. **15**(10): p. 1572-81.
7. Liu, Y., et al., *Autophagy regulates programmed cell death during the plant innate immune response.* Cell, 2005. **121**(4): p. 567-77.
8. Nakagawa, I., et al., *Autophagy defends cells against invading group A Streptococcus.* Science, 2004. **306**(5698): p. 1037-40.
9. Andrade, R.M., et al., *CD40 induces macrophage anti-Toxoplasma gondii activity by triggering autophagy-dependent fusion of pathogen-containing vacuoles and lysosomes.* J Clin Invest, 2006. **116**(9): p. 2366-77.
10. Gutierrez, M.G., et al., *Protective role of autophagy against Vibrio cholerae cytolysin, a pore-forming toxin from V. cholerae.* Proc Natl Acad Sci U S A, 2007. **104**(6): p. 1829-34.
11. Schmid, D. and C. Munz, *Innate and adaptive immunity through autophagy.* Immunity, 2007. **27**(1): p. 11-21.
12. Mareninova, O.A., et al., *Impaired autophagic flux mediates acinar cell vacuole formation and trypsinogen activation in rodent models of acute pancreatitis.* J Clin Invest, 2009. **119**(11): p. 3340-55.
13. Nixon, R.A., et al., *Extensive involvement of autophagy in Alzheimer disease: an immuno-electron microscopy study.* J Neuropathol Exp Neurol, 2005. **64**(2): p. 113-22.
14. Mathew, R., V. Karantza-Wadsworth, and E. White, *Role of autophagy in cancer.* Nat Rev Cancer, 2007. **7**(12): p. 961-7.
15. Ramser, B., et al., *Hydroxychloroquine modulates metabolic activity and proliferation and induces autophagic cell death of human dermal fibroblasts.* J Invest Dermatol, 2009. **129**(10): p. 2419-26.
16. Xu, Y., et al., *Autophagy contributes to caspase-independent macrophage cell death.* J Biol Chem, 2006. **281**(28): p. 19179-87.
17. Yu, L., et al., *Autophagic programmed cell death by selective catalase degradation.* Proc Natl Acad Sci U S A, 2006. **103**(13): p. 4952-7.
18. Yu, L., et al., *Regulation of an ATG7-beclin 1 program of autophagic cell death by caspase-8.* Science, 2004. **304**(5676): p. 1500-2.
19. Mizushima, N., *Methods for monitoring autophagy.* Int J Biochem Cell Biol, 2004. **36**(12): p. 2491-502.
20. Shintani, T. and D.J. Klionsky, *Autophagy in health and disease: a double-edged sword.* Science, 2004. **306**(5698): p. 990-5.
21. Longatti, A. and S.A. Tooze, *Vesicular trafficking and autophagosome formation.* Cell Death Differ, 2009. **16**(7): p. 956-65.

22. Petiot, A., et al., *Distinct classes of phosphatidylinositol 3'-kinases are involved in signaling pathways that control macroautophagy in HT-29 cells.* J Biol Chem, 2000. **275**(2): p. 992-8.
23. Obara, K. and Y. Ohsumi, *Dynamics and function of PtdIns(3)P in autophagy.* Autophagy, 2008. **4**(7): p. 952-4.
24. Blommaart, E.F., et al., *The phosphatidylinositol 3-kinase inhibitors wortmannin and LY294002 inhibit autophagy in isolated rat hepatocytes.* Eur J Biochem, 1997. **243**(1-2): p. 240-6.
25. Klionsky, D.J., et al., *Guidelines for the use and interpretation of assays for monitoring autophagy in higher eukaryotes.* Autophagy, 2008. **4**(2): p. 151-75.
26. Fader, C.M. and M.I. Colombo, *Autophagy and multivesicular bodies: two closely related partners.* Cell Death Differ, 2009. **16**(1): p. 70-8.
27. Mellman, I., *Endocytosis and molecular sorting.* Annu Rev Cell Dev Biol, 1996. **12**: p. 575-625.
28. Stoorvogel, W., et al., *Late endosomes derive from early endosomes by maturation.* Cell, 1991. **65**(3): p. 417-27.
29. Luzio, J.P., P.R. Pryor, and N.A. Bright, *Lysosomes: fusion and function.* Nat Rev Mol Cell Biol, 2007. **8**(8): p. 622-32.
30. Uchil, P. and W. Mothes, *Viral entry: a detour through multivesicular bodies.* Nat Cell Biol, 2005. **7**(7): p. 641-2.
31. Chow, A., et al., *Dendritic cell maturation triggers retrograde MHC class II transport from lysosomes to the plasma membrane.* Nature, 2002. **418**(6901): p. 988-94.
32. Kleijmeer, M., et al., *Reorganization of multivesicular bodies regulates MHC class II antigen presentation by dendritic cells.* J Cell Biol, 2001. **155**(1): p. 53-63.
33. Murk, J.L., et al., *Endosomal compartmentalization in three dimensions: implications for membrane fusion.* Proc Natl Acad Sci U S A, 2003. **100**(23): p. 13332-7.
34. Levine, B. and D.J. Klionsky, *Development by self-digestion: molecular mechanisms and biological functions of autophagy.* Dev Cell, 2004. **6**(4): p. 463-77.
35. Ostrowicz, C.W., C.T. Meiringer, and C. Ungermann, *Yeast vacuole fusion: a model system for eukaryotic endomembrane dynamics.* Autophagy, 2008. **4**(1): p. 5-19.
36. Jahn, R. and T.C. Sudhof, *Membrane fusion and exocytosis.* Annu Rev Biochem, 1999. **68**: p. 863-911.
37. Baumert, M., et al., *Synaptobrevin: an integral membrane protein of 18,000 daltons present in small synaptic vesicles of rat brain.* EMBO J, 1989. **8**(2): p. 379-84.
38. Stow, J.L., A.P. Manderson, and R.Z. Murray, *SNAREing immunity: the role of SNAREs in the immune system.* Nat Rev Immunol, 2006. **6**(12): p. 919-29.
39. Hanson, P.I., J.E. Heuser, and R. Jahn, *Neurotransmitter release - four years of SNARE complexes.* Curr Opin Neurobiol, 1997. **7**(3): p. 310-5.
40. Lang, T., et al., *SNAREs are concentrated in cholesterol-dependent clusters that define docking and fusion sites for exocytosis.* EMBO J, 2001. **20**(9): p. 2202-13.
41. Ishihara, N., et al., *Autophagosome requires specific early Sec proteins for its formation and NSF/SNARE for vacuolar fusion.* Mol Biol Cell, 2001. **12**(11): p. 3690-702.
42. Atlashkin, V., et al., *Deletion of the SNARE vti1b in mice results in the loss of a single SNARE partner, syntaxin 8.* Mol Cell Biol, 2003. **23**(15): p. 5198-207.
43. Takenouchi, T., et al., *The activation of P2X7 receptor impairs lysosomal functions and stimulates the release of autophagolysosomes in microglial cells.* J Immunol, 2009. **182**(4): p. 2051-62.
44. Abeliovich, H. and D.J. Klionsky, *Autophagy in yeast: mechanistic insights and physiological function.* Microbiol Mol Biol Rev, 2001. **65**(3): p. 463-79, table of contents.
45. Komatsu, M., E. Kominami, and K. Tanaka, *Autophagy and neurodegeneration.* Autophagy, 2006. **2**(4): p. 315-7.

46. Hara, T., et al., *Suppression of basal autophagy in neural cells causes neurodegenerative disease in mice.* Nature, 2006. **441**(7095): p. 885-9.
47. Yu, W.H., et al., *Macroautophagy--a novel Beta-amyloid peptide-generating pathway activated in Alzheimer's disease.* J Cell Biol, 2005. **171**(1): p. 87-98.
48. Karantza-Wadsworth, V., et al., *Autophagy mitigates metabolic stress and genome damage in mammary tumorigenesis.* Genes Dev, 2007. **21**(13): p. 1621-35.
49. Komatsu, M., et al., *Loss of autophagy in the central nervous system causes neurodegeneration in mice.* Nature, 2006. **441**(7095): p. 880-4.
50. Komatsu, M., et al., *Homeostatic levels of p62 control cytoplasmic inclusion body formation in autophagy-deficient mice.* Cell, 2007. **131**(6): p. 1149-63.
51. Cunningham, T.J., *Naturally occurring neuron death and its regulation by developing neural pathways.* Int Rev Cytol, 1982. **74**: p. 163-86.
52. Clarke, P.G., *Developmental cell death: morphological diversity and multiple mechanisms.* Anat Embryol (Berl), 1990. **181**(3): p. 195-213.
53. Schweichel, J.U. and H.J. Merker, *The morphology of various types of cell death in prenatal tissues.* Teratology, 1973. **7**(3): p. 253-66.
54. Fan, T.J., et al., *Caspase family proteases and apoptosis.* Acta Biochim Biophys Sin (Shanghai), 2005. **37**(11): p. 719-27.
55. Salvesen, G.S. and V.M. Dixit, *Caspases: intracellular signaling by proteolysis.* Cell, 1997. **91**(4): p. 443-6.
56. Rao, R.V., et al., *Coupling endoplasmic reticulum stress to the cell death program. An Apaf-1-independent intrinsic pathway.* J Biol Chem, 2002. **277**(24): p. 21836-42.
57. Morishima, N., et al., *An endoplasmic reticulum stress-specific caspase cascade in apoptosis. Cytochrome c-independent activation of caspase-9 by caspase-12.* J Biol Chem, 2002. **277**(37): p. 34287-94.
58. Luo, X., et al., *Bid, a Bcl2 interacting protein, mediates cytochrome c release from mitochondria in response to activation of cell surface death receptors.* Cell, 1998. **94**(4): p. 481-90.
59. Finucane, D.M., et al., *Bax-induced caspase activation and apoptosis via cytochrome c release from mitochondria is inhibitable by Bcl-xL.* J Biol Chem, 1999. **274**(4): p. 2225-33.
60. Vakkila, J. and M.T. Lotze, *Inflammation and necrosis promote tumour growth.* Nat Rev Immunol, 2004. **4**(8): p. 641-8.
61. Golstein, P. and G. Kroemer, *Cell death by necrosis: towards a molecular definition.* Trends Biochem Sci, 2007. **32**(1): p. 37-43.
62. Uchiyama, Y., *Autophagic cell death and its execution by lysosomal cathepsins.* Arch Histol Cytol, 2001. **64**(3): p. 233-46.
63. Tanida, I., et al., *The human homolog of Saccharomyces cerevisiae Apg7p is a Protein-activating enzyme for multiple substrates including human Apg12p, GATE-16, GABARAP, and MAP-LC3.* J Biol Chem, 2001. **276**(3): p. 1701-6.
64. Jiang, Z., et al., *Frequency and distribution of DNA fragmentation as a marker of cell death in chronic liver diseases.* Virchows Arch, 1997. **431**(3): p. 189-94.
65. Tanida, I., et al., *Human Apg3p/Aut1p homologue is an authentic E2 enzyme for multiple substrates, GATE-16, GABARAP, and MAP-LC3, and facilitates the conjugation of hApg12p to hApg5p.* J Biol Chem, 2002. **277**(16): p. 13739-44.
66. Ohmuraya, M., et al., *Autophagic cell death of pancreatic acinar cells in serine protease inhibitor Kazal type 3-deficient mice.* Gastroenterology, 2005. **129**(2): p. 696-705.
67. Bhoopathi, P., et al., *Cathepsin B facilitates autophagy-mediated apoptosis in SPARC overexpressed primitive neuroectodermal tumor cells.* Cell Death Differ, 2010.

68. Ma, Y., et al., *NF-kappaB protects macrophages from lipopolysaccharide-induced cell death: the role of caspase 8 and receptor-interacting protein.* J Biol Chem, 2005. **280**(51): p. 41827-34.
69. Kim, H.Y., et al., *Upregulation of LPS-induced chemokine KC expression by 15-deoxy-delta12,14-prostaglandin J2 in mouse peritoneal macrophages.* Immunol Cell Biol, 2005. **83**(3): p. 286-93.
70. Lin, Y., et al., *Cleavage of the death domain kinase RIP by caspase-8 prompts TNF-induced apoptosis.* Genes Dev, 1999. **13**(19): p. 2514-26.
71. Lee, C.Y. and E.H. Baehrecke, *Steroid regulation of autophagic programmed cell death during development.* Development, 2001. **128**(8): p. 1443-55.
72. Berry, D.L. and E.H. Baehrecke, *Growth arrest and autophagy are required for salivary gland cell degradation in Drosophila.* Cell, 2007. **131**(6): p. 1137-48.
73. Almeida, P.C., et al., *Cathepsin B activity regulation. Heparin-like glycosaminogylcans protect human cathepsin B from alkaline pH-induced inactivation.* J Biol Chem, 2001. **276**(2): p. 944-51.
74. Mohamed, M.M. and B.F. Sloane, *Cysteine cathepsins: multifunctional enzymes in cancer.* Nat Rev Cancer, 2006. **6**(10): p. 764-75.
75. Benchoua, A., et al., *Activation of proinflammatory caspases by cathepsin B in focal cerebral ischemia.* J Cereb Blood Flow Metab, 2004. **24**(11): p. 1272-9.
76. Mort, J.S., A.D. Recklies, and A.R. Poole, *Extracellular presence of the lysosomal proteinase cathepsin B in rheumatoid synovium and its activity at neutral pH.* Arthritis Rheum, 1984. **27**(5): p. 509-15.
77. Willingham, S.B. and J.P. Ting, *NLRs and the dangers of pollution and aging.* Nat Immunol, 2008. **9**(8): p. 831-3.
78. Lah, T.T., et al., *Degradation of laminin by human tumor cathepsin B.* Clin Exp Metastasis, 1989. **7**(4): p. 461-8.
79. Mai, J., D.M. Waisman, and B.F. Sloane, *Cell surface complex of cathepsin B/annexin II tetramer in malignant progression.* Biochim Biophys Acta, 2000. **1477**(1-2): p. 215-30.
80. Eeckhout, Y. and G. Vaes, *Further studies on the activation of procollagenase, the latent precursor of bone collagenase. Effects of lysosomal cathepsin B, plasmin and kallikrein, and spontaneous activation.* Biochem J, 1977. **166**(1): p. 21-31.
81. Kobayashi, H., et al., *Cathepsin B efficiently activates the soluble and the tumor cell receptor-bound form of the proenzyme urokinase-type plasminogen activator (Pro-uPA).* J Biol Chem, 1991. **266**(8): p. 5147-52.
82. Poole, A.R., et al., *Differences in secretion of the proteinase cathepsin B at the edges of human breast carcinomas and fibroadenomas.* Nature, 1978. **273**(5663): p. 545-7.
83. Lotem, J., et al., *Cellular oxidative stress and the control of apoptosis by wild-type p53, cytotoxic compounds, and cytokines.* Proc Natl Acad Sci U S A, 1996. **93**(17): p. 9166-71.
84. Guicciardi, M.E., et al., *Cathepsin B contributes to TNF-alpha-mediated hepatocyte apoptosis by promoting mitochondrial release of cytochrome c.* J Clin Invest, 2000. **106**(9): p. 1127-37.
85. Werneburg, N.W., et al., *Tumor necrosis factor-alpha-associated lysosomal permeabilization is cathepsin B dependent.* Am J Physiol Gastrointest Liver Physiol, 2002. **283**(4): p. G947-56.
86. Takeshige, K., et al., *Autophagy in yeast demonstrated with proteinase-deficient mutants and conditions for its induction.* J Cell Biol, 1992. **119**(2): p. 301-11.
87. Felbor, U., et al., *Neuronal loss and brain atrophy in mice lacking cathepsins B and L.* Proc Natl Acad Sci U S A, 2002. **99**(12): p. 7883-8.
88. Ha, S.D., et al., *Cathepsin B is involved in the trafficking of TNF-alpha-containing vesicles to the plasma membrane in macrophages.* J Immunol, 2008. **181**(1): p. 690-7.
89. Halangk, W., et al., *Role of cathepsin B in intracellular trypsinogen activation and the onset of acute pancreatitis.* J Clin Invest, 2000. **106**(6): p. 773-81.

90. Wesche, J., et al., *Characterization of membrane translocation by anthrax protective antigen.* Biochemistry, 1998. **37**(45): p. 15737-46.
91. Miller, C.J., J.L. Elliott, and R.J. Collier, *Anthrax protective antigen: prepore-to-pore conversion.* Biochemistry, 1999. **38**(32): p. 10432-41.
92. Kim, S.O., et al., *Orphan nuclear receptor Nur77 is involved in caspase-independent macrophage cell death.* J Exp Med, 2003. **197**(11): p. 1441-52.
93. Mathison, J.C., E. Wolfson, and R.J. Ulevitch, *Participation of tumor necrosis factor in the mediation of gram negative bacterial lipopolysaccharide-induced injury in rabbits.* J Clin Invest, 1988. **81**(6): p. 1925-37.
94. Mosmann, T., *Rapid colorimetric assay for cellular growth and survival: application to proliferation and cytotoxicity assays.* J Immunol Methods, 1983. **65**(1-2): p. 55-63.
95. Ha, S.D., et al., *Cathepsin B-mediated autophagy flux facilitates the anthrax toxin receptor 2-mediated delivery of anthrax lethal factor into the cytoplasm.* J Biol Chem, 2010. **285**(3): p. 2120-9.
96. Blom, T.S., et al., *Defective endocytic trafficking of NPC1 and NPC2 underlying infantile Niemann-Pick type C disease.* Hum Mol Genet, 2003. **12**(3): p. 257-72.
97. Liao, G., et al., *Cholesterol accumulation is associated with lysosomal dysfunction and autophagic stress in Npc1 -/- mouse brain.* Am J Pathol, 2007. **171**(3): p. 962-75.
98. Lajoie, P., et al., *The lipid composition of autophagic vacuoles regulates expression of multilamellar bodies.* J Cell Sci, 2005. **118**(Pt 9): p. 1991-2003.
99. Koh, C.H. and N.S. Cheung, *Cellular mechanism of U18666A-mediated apoptosis in cultured murine cortical neurons: bridging Niemann-Pick disease type C and Alzheimer's disease.* Cell Signal, 2006. **18**(11): p. 1844-53.
100. Sobo, K., et al., *Late endosomal cholesterol accumulation leads to impaired intra-endosomal trafficking.* PLoS One, 2007. **2**(9): p. e851.
101. Ohtani, Y., et al., *Differential effects of alpha-, beta- and gamma-cyclodextrins on human erythrocytes.* Eur J Biochem, 1989. **186**(1-2): p. 17-22.
102. Chintagari, N.R., et al., *Effect of cholesterol depletion on exocytosis of alveolar type II cells.* Am J Respir Cell Mol Biol, 2006. **34**(6): p. 677-87.
103. Cheng, J., et al., *Cholesterol depletion induces autophagy.* Biochem Biophys Res Commun, 2006. **351**(1): p. 246-52.
104. Murray, R.Z., et al., *Syntaxin 6 and Vti1b form a novel SNARE complex, which is up-regulated in activated macrophages to facilitate exocytosis of tumor necrosis Factor-alpha.* J Biol Chem, 2005. **280**(11): p. 10478-83.
105. Pagan, J.K., et al., *The t-SNARE syntaxin 4 is regulated during macrophage activation to function in membrane traffic and cytokine secretion.* Curr Biol, 2003. **13**(2): p. 156-60.
106. Pombo, I., et al., *IgE receptor type I-dependent regulation of a Rab3D-associated kinase: a possible link in the calcium-dependent assembly of SNARE complexes.* J Biol Chem, 2001. **276**(46): p. 42893-900.
107. Hepp, R., et al., *Phosphorylation of SNAP-23 regulates exocytosis from mast cells.* J Biol Chem, 2005. **280**(8): p. 6610-20.
108. Jutras, I. and T.L. Reudelhuber, *Prorenin processing by cathepsin B in vitro and in transfected cells.* FEBS Lett, 1999. **443**(1): p. 48-52.
109. Dunn, A.D. and J.T. Dunn, *Cysteine proteinases from human thyroids and their actions on thyroglobulin.* Endocrinology, 1988. **123**(2): p. 1089-97.
110. Hill, P.A., et al., *Inhibition of bone resorption by selective inactivators of cysteine proteinases.* J Cell Biochem, 1994. **56**(1): p. 118-30.

111. Paludan, C., et al., *Endogenous MHC class II processing of a viral nuclear antigen after autophagy.* Science, 2005. **307**(5709): p. 593-6.
112. Morton, P.A., et al., *Delivery of nascent MHC class II-invariant chain complexes to lysosomal compartments and proteolysis of invariant chain by cysteine proteases precedes peptide binding in B-lymphoblastoid cells.* J Immunol, 1995. **154**(1): p. 137-50.
113. Karten, B., K.B. Peake, and J.E. Vance, *Mechanisms and consequences of impaired lipid trafficking in Niemann-Pick type C1-deficient mammalian cells.* Biochim Biophys Acta, 2009. **1791**(7): p. 659-70.
114. Ishibashi, S., T. Yamazaki, and K. Okamoto, *Association of autophagy with cholesterol-accumulated compartments in Niemann-Pick disease type C cells.* J Clin Neurosci, 2009. **16**(7): p. 954-9.
115. Fengsrud, M., et al., *Ultrastructural and immunocytochemical characterization of autophagic vacuoles in isolated hepatocytes: effects of vinblastine and asparagine on vacuole distributions.* Exp Cell Res, 1995. **221**(2): p. 504-19.
116. Pacheco, C.D. and A.P. Lieberman, *The pathogenesis of Niemann-Pick type C disease: a role for autophagy?* Expert Rev Mol Med, 2008. **10**: p. e26.
117. Kim, Y.S., et al., *TNF-induced activation of the Nox1 NADPH oxidase and its role in the induction of necrotic cell death.* Mol Cell, 2007. **26**(5): p. 675-87.
118. Wu, Y.T., et al., *Dual role of 3-methyladenine in modulation of autophagy via different temporal patterns of inhibition on class I and III phosphoinositide 3-kinase.* J Biol Chem, 2010. **285**(14): p. 10850-61.
119. Nakagawa, T., et al., *Cyclophilin D-dependent mitochondrial permeability transition regulates some necrotic but not apoptotic cell death.* Nature, 2005. **434**(7033): p. 652-8.
120. Degterev, A., et al., *Chemical inhibitor of nonapoptotic cell death with therapeutic potential for ischemic brain injury.* Nat Chem Biol, 2005. **1**(2): p. 112-9.
121. Shim, J.H., et al., *Protective effect of oxidative stress in HaCaT keratinocytes expressing E7 oncogene.* Amino Acids, 2008. **34**(1): p. 135-41.
122. Rushworth, S.A. and D.J. MacEwan, *HO-1 underlies resistance of AML cells to TNF-induced apoptosis.* Blood, 2008. **111**(7): p. 3793-801.
123. Broker, L.E., et al., *Cathepsin B mediates caspase-independent cell death induced by microtubule stabilizing agents in non-small cell lung cancer cells.* Cancer Res, 2004. **64**(1): p. 27-30.
124. Boyden, E.D. and W.F. Dietrich, *Nalp1b controls mouse macrophage susceptibility to anthrax lethal toxin.* Nat Genet, 2006. **38**(2): p. 240-4.
125. Chapelsky, S., et al., *Inhibition of anthrax lethal toxin-induced cytolysis of RAW264.7 cells by celastrol.* PLoS One, 2008. **3**(1): p. e1421.
126. Guillon-Munos, A., M.X. van Bemmelen, and P.G. Clarke, *Role of phosphoinositide 3-kinase in the autophagic death of serum-deprived PC12 cells.* Apoptosis, 2005. **10**(5): p. 1031-41.
127. Schamberger, C.J., C. Gerner, and C. Cerni, *Caspase-9 plays a marginal role in serum starvation-induced apoptosis.* Exp Cell Res, 2005. **302**(1): p. 115-28.
128. Eykelbosh, A.J. and G. Van Der Kraak, *A role for the lysosomal protease cathepsin B in zebrafish follicular apoptosis.* Comp Biochem Physiol A Mol Integr Physiol, 2010. **156**(2): p. 218-23.
129. Dixon, T.C., et al., *Anthrax.* N Engl J Med, 1999. **341**(11): p. 815-26.
130. Mikesell, P., et al., *Evidence for plasmid-mediated toxin production in Bacillus anthracis.* Infect Immun, 1983. **39**(1): p. 371-6.
131. Bradley, K.A., et al., *Identification of the cellular receptor for anthrax toxin.* Nature, 2001. **414**(6860): p. 225-9.
132. Scobie, H.M., et al., *Human capillary morphogenesis protein 2 functions as an anthrax toxin receptor.* Proc Natl Acad Sci U S A, 2003. **100**(9): p. 5170-4.

133. Scobie, H.M. and J.A. Young, *Interactions between anthrax toxin receptors and protective antigen.* Curr Opin Microbiol, 2005. **8**(1): p. 106-12.
134. Abrami, L., S.H. Leppla, and F.G. van der Goot, *Receptor palmitoylation and ubiquitination regulate anthrax toxin endocytosis.* J Cell Biol, 2006. **172**(2): p. 309-20.
135. Rainey, G.J., et al., *Receptor-specific requirements for anthrax toxin delivery into cells.* Proc Natl Acad Sci U S A, 2005. **102**(37): p. 13278-83.
136. Wolfe, J.T., et al., *Whole-cell voltage clamp measurements of anthrax toxin pore current.* J Biol Chem, 2005. **280**(47): p. 39417-22.
137. Almeida, P.C., et al., *Hydrolysis by plasma kallikrein of fluorogenic peptides derived from prorenin processing site.* Biochim Biophys Acta, 2000. **1479**(1-2): p. 83-90.
138. Illy, C., et al., *Role of the occluding loop in cathepsin B activity.* J Biol Chem, 1997. **272**(2): p. 1197-202.
139. Mayer, R.J. and F. Doherty, *Intracellular protein catabolism: state of the art.* FEBS Lett, 1986. **198**(2): p. 181-93.
140. Chen, Y.A. and R.H. Scheller, *SNARE-mediated membrane fusion.* Nat Rev Mol Cell Biol, 2001. **2**(2): p. 98-106.
141. Scales, S.J., et al., *SNAREs contribute to the specificity of membrane fusion.* Neuron, 2000. **26**(2): p. 457-64.
142. Creutz, C.E., *The annexins and exocytosis.* Science, 1992. **258**(5084): p. 924-31.
143. Jacob, R., et al., *Annexin II is required for apical transport in polarized epithelial cells.* J Biol Chem, 2004. **279**(5): p. 3680-4.
144. Huang, J., et al., *Annexin II is a thiazolidinedione-responsive gene involved in insulin-induced glucose transporter isoform 4 translocation in 3T3-L1 adipocytes.* Endocrinology, 2004. **145**(4): p. 1579-86.
145. Knight, D.E. and P.F. Baker, *Calcium-dependence of catecholamine release from bovine adrenal medullary cells after exposure to intense electric fields.* J Membr Biol, 1982. **68**(2): p. 107-40.